EFFECTS OF POLISHING SHOT-PEENED SURFACES ON FRETTING FATIGUE BEHAVIOR OF Ti-6Al-4V

THESIS

Kasey Scheel, ENS, USN

AFIT/GAE/ENY/06-S10

DEPARTMENT OF THE AIR FORCE
AIR UNIVERSITY

AIR FORCE INSTITUTE OF TECHNOLOGY

Wright-Patterson Air Force Base, Ohio

The views expressed in this thesis are those of the author and do not reflect the official policy or position of the United States Air Force, Department of Defense, or the United States Government.

AFIT/GAE/ENY/06-S10

EFFECTS OF POLISHING SHOT-PEENED SURFACES ON FRETTING FATIGUE BEHAVIOR OF Ti-6Al-4V

THESIS

Presented to the Faculty

Department of Aeronautical and Astronautical Engineering

Graduate School of Engineering and Management

Air Force Institute of Technology

Air University

Air Education And Training Command

In Partial Fulfillment of the Requirements for the

Degree of Master of Science in Aeronautical Engineering

Kasey S. Scheel, B.S.

ENSIGN, USN

September 2006

Abstract

The research of this thesis was done to investigate the effects of polishing a shot-peened specimen of Ti-6Al-4V on the fretting fatigue life. The shot-peening process, though one of the most beneficial techniques in prolonging fretting fatigue life, creates a textured surface that may lead to problems on the micro level. This research was done in an attempt to further improve the peening process by examining the effects of another surface treatment to be used in conjunction, surface polishing. The rough peened surface may contain abrupt changes in surface geometry that act as stress risers, which are more highly prone to crack initiation. Specimens were hand polished after they were peened to remove approximately 25 microns of material from the surface to remove all stress risers while preserving the beneficial residual stresses created by peening. Experiments designed to simulate fretting fatigue similar to previous research were conducted until specimens fractured. Seven experiments were conducted using titanium allow Ti-6Al-4V, shot peened using 7A intensity. All tests were run at ambient air temperature. Fatigue parameters, such as stress range and effective stress, were analyzed. Fretting fatigue conditions were determined and surface roughness measurements of polished and unpolished specimens were taken. It was concluded that, though fatigue life was improved over that of un-peened specimens, the polishing process did not improve the fretting fatigue life of the alloy.

Acknowledgements

I would like to express my sincere appreciation to my faculty advisor and my thesis advisor Dr. Mall for his guidance and support throughout this thesis project. A word of thanks is owed to those who served on the thesis defense committee as well, Dr. Vinod Jain at the University of Dayton and Dr. Michael Heil at AFIT, for their patience and understanding. I would also like to thank my sponsor, Dr. Mark Blodgett at AFRL/MLLP. In addition, there were many who provided assistance along the way. I would like to thank the laboratory technicians, Barry Page and John Hixenbaugh. Those at the machine shop provided invaluable service in preparing equipment and specimens for testing and did so in a timely manner. For that I am grateful.

Table of Contents

Page

List of Figures

Page

Page

List of Tables

Page

List of Variables

f	coefficient of friction
Q	tangential load
P	contact load
$\varepsilon_f^{'}$	fatigue ductility coefficient
N_f	number of stain reversals to failure
c’	fatigue ductility exponent
$(\sigma_T)_{\max}$	maximum tangential stress
$(\tau\delta)_{\max}$	maximum frictional work
p(x)	pressure distribution
σ_{axial}	axial stress
σ_R	fretting fatigue strength reduction
p_0	maximum pressure experienced due to the normal load
w(x)	weight function
E	Young’s Modulus
u	slip distance
a	contact half length
d	specimen thickness
b	specimen half thickness
c	stick zone half length
r	fretting pad radius

R	stress ratio
υ	Poisson's ratio
q(x)	shear stress distribution
$(\sigma_{xx})_{contact}$	axial stress due to contact load
ε_{xx}	axial strain
$(\sigma_{xx})_{\tan gential}$	axial stress due to tangential load
σ_{eff}	effective stress
R_a	surface roughness
R_q	root mean squared surface roughness

EFFECTS OF POLISHING SHOT-PEENED SURFACES ON FRETTING FATIGUE BEHAVIOR OF Ti-6Al-4V

1 Introduction

1.1 Fretting Fatigue Problem

Fretting fatigue is a surface phenomenon. Fretting occurs when any junction or interface between two components is subjected to some oscillating force, or cyclic loading, and is a much more aggressive form of crack initiation than that prevalent at a free surface. This condition occurs most frequently in bolted or otherwise mechanically fastened joints. In cases where an oscillating tensile load is experienced in addition to contact forces, accelerated crack propagation often results. This phenomenon, known as fretting fatigue, occurs frequently and is a regular source of premature failure even in components of high integrity. Since it is quite difficult to measure crack growth rate beneath a fretting contact, fretting fatigue performance is typically assessed by measuring the total life of the specimen [1]. Fretting fatigue is a common cause of failure in turbine engines and is therefore of great interest to the aerospace industry. This source of fatigue commonly occurs at the interface of certain components such as the disk slot and blade attachment of turbine engines and is a frequent source of component failure. Fretting fatigue leads to both premature failure and increased maintenance costs because of the shortened lifespan of the components. It is generally agreed upon among researchers that numerous factors contribute, either independently or jointly, to fretting fatigue. However, the individual contribution of each factor to the overall fatigue of the material is not understood. The most substantial contributing factors to fretting fatigue are thought to be material properties, environmental conditions, applied stresses and displacement and contact pressure between contact surfaces.

Some of these variables directly influence each other. For example, increasing the magnitude of the applied contact load increases the area of contact between the fretting surfaces and the local and peak pressure, all other variables being held constant. Therefore, ongoing research is being done to better understand the individual impact of these parameters on fretting fatigue [2]. Currently, there is no reliable way to predict failure due to fretting fatigue nor can fretting fatigue be accounted for in preliminary stages of engine design. Consequently, engineers must incorporate large factors of safety into such designs to account for the potential of fretting fatigue failure, making these engine components more robust than may be necessary. This design results in heavier, more expensive, less efficient engines. Further understanding of the intricacies of fretting fatigue will enable engineers to better predict and prevent failure, thus greatly increasing the efficiency of the design and maintenance processes. In general, there are a number of reasons for the engineering community to study and understand the challenges presented by fretting fatigue, some of which are:

1) By understanding this detriment to various mechanical processes, it becomes more feasible for the engineering community to alleviate and prevent it.
2) Maintenance, inspection, and replacement schedules are determined in part by our understanding of fretting mechanisms.
3) The necessary development of standardized experimental procedures for fretting fatigue demand continuing growth in our knowledge of this subject matter [3].

1.2 Shot-Peening in Fretting Fatigue

The purpose of this study is to understand the effects of surface treatments on high-cycle fretting fatigue life of Ti-6Al-4V. Shot-peening, a common type of surface commonly used to increase resistance to fretting fatigue, is a process in which the surface of interest, in this case Ti-6Al-4V, is bombarded with small, hard particles, generally having diameters of 0.1-

1.0 mm, traveling at high velocity. This creates localized plastic deformation within the outer surface region. Shot-peening changes the physical and mechanical properties of the material, creating a residual compressive stress on the material surface which is opposed by a residual tensile stress within the material. This induced compressive stress typically reaches a depth of between one-quarter and one-half of the shot diameter and plays a critical role in crack initiation and propagation retardation [4]. It also changes the surface roughness of the material which affects the coefficient of friction of the material. In addition, distortion of the grains near the surface of the material caused by shot-peening reduces the susceptibility of crack propagation in this region. It is accepted that shot-peening improves fatigue life, strength operation and corrosion resistance. It can also close pre-existing cracks if the residual compressive stress reaches a depth greater than that of the crack. However, if the peening is too intense it can have an adverse effect, perhaps creating a brittle material with a higher notch sensitivity [5]. It is important to note that the alteration of these properties varies depending on shot-peening intensity. As expected, the depth of the boundary between tensile and compressive stresses is directly related to shot-peening intensity. However, it has been observed that an increase in peening intensity has negligible effects on the maximum residual compressive stress on the material surface [6].

1.3 Objectives

The purpose of this study was similar to that of many others in that the effects of peening processes on high-cycle fretting fatigue of Ti-6Al-4V were of primary interest. However, unlike previous experimentation, the increased surface roughness associated with shot-peened surfaces was removed by hand-polishing the contact surfaces, removing approximately one one-thousandth of an inch of material from each surface of the test specimens. This was done in an attempt to eliminate any local stress raisers that may have

been created as a result of the peening process. The results were compared to previous experimental results to determine if any improvement in fretting fatigue life was made.

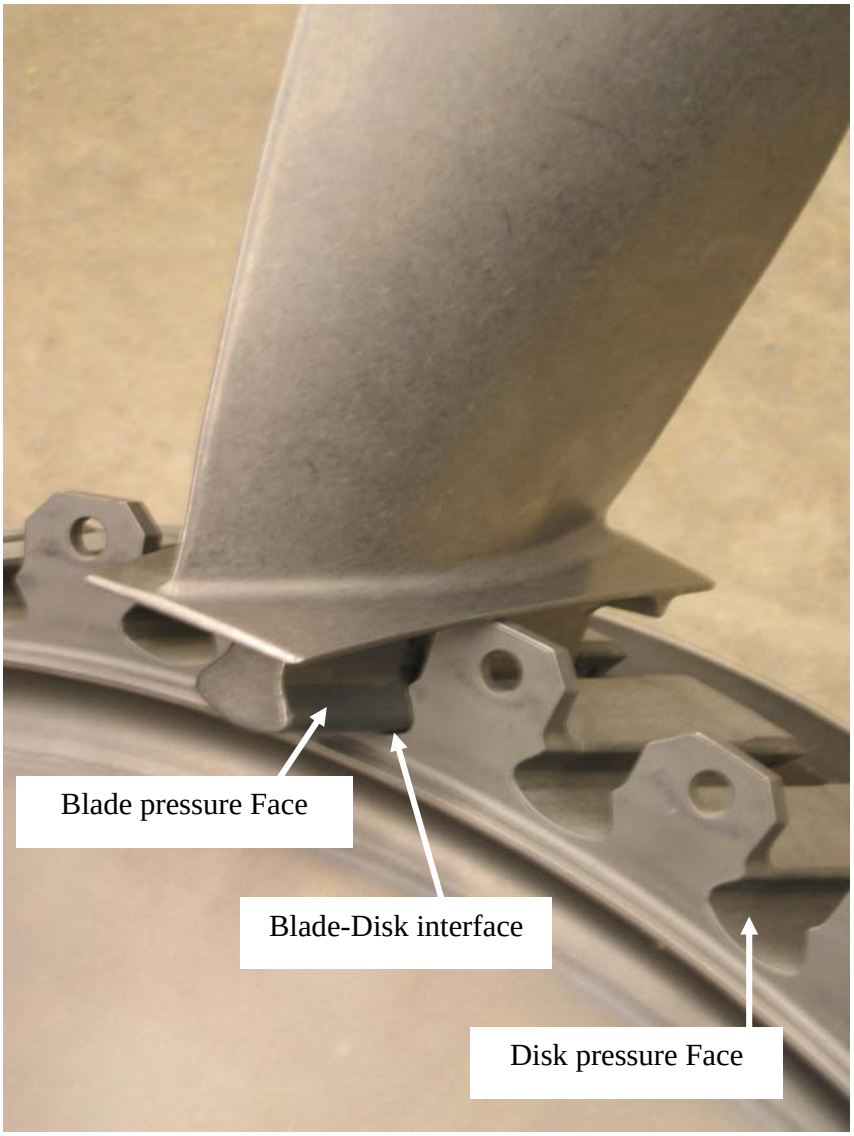

Figure 1.1. Blade/disc dovetail joint of a turbine engine.

2 Background

Equation Section 2

2.1 2.1 Variables Affecting Fretting Fatigue

From the first identification of fretting fatigue in the early 20th century until recently, fretting was thought to be a purely mechanical process. Currently there are numerous studies supporting the theory that fretting is a chemical as well as mechanical process. Waterhouse [7] categorized the variables affecting fretting fatigue life into three factions; mechanical, physical and environmental influences.

Mechanical variables include but are not limited to number of cycles, frequency, normal load and amplitude of slip. The coefficient of friction, which generally depends on the applied contact load, is another. Lee [8] stated that 10,000-15,000 fretting fatigue cycles must be completed before a stabilized coefficient of friction (f) could be determined using the simple formula: $f = \frac{Q}{P}$, where Q is the tangential load and P is the applied contact load. His research showed that this coefficient ranged from 0.33~0.46 for shot-peened Ti-6Al-4V and from 0.37~0.46 for un-peened Ti-6Al-4V, showing no significant affect on the friction coefficient. Other research [9, 10] showed that, when comparing the effects of varying coefficients of friction, an increase from 0.45 to 0.70, equivalent to a 66% increase, caused minimal effects on other fretting fatigue variables. Specifically, a 20% increase in strain range was measured. This finding indicates that it is practical to approximate the coefficient of friction as constant.

Contact pad geometry effects were investigated by Namjoshi, et al [11, 12] using un-peened Ti-6Al-4V specimens. They used cylindrical pad geometry of different radii as well as flat pad geometry with filleted corners. In all cases, it was shown that fretting fatigue life

was significantly less than plain fatigue life. Fretting fatigue life was also shown to strongly depend on pad geometry. Similar dependence was found when looking at axial load frequency and contact pressure. Iyer, et al. [13] showed that increasing axial load frequency from 1 Hertz (Hz) to 200 Hz while keeping the contact load constant reduced fretting fatigue life. Additionally, it was observed that increasing the contact load while maintaining a constant axial load frequency also reduced fatigue life. Interestingly, an increase in the contact pressure while maintaining an axial load frequency of 200 Hz did not appear to have significant impact on fretting fatigue life.

Some physical properties include temperature, relative surface hardness and surface finish. Lee, et al. [6, 14] investigated fretting fatigue life of peened and un-peened Ti-6Al-4V at elevated temperatures, up to $260°C$. Experiments showed that at $260°C$, shot-peening no longer had an advantageous effect on fretting fatigue life. That is, it did not aid to prolong fatigue life as compared to un-peened specimens at the same temperature and therefore logically resulted in a fatigue life much shorter than shot-peened Ti-6Al-4V at room temperature. This was attributed to the stress relaxation associated with elevated temperatures. For un-peened specimens, a raise in temperature had no effect on fretting fatigue life.

Environmental conditions include any natural or atmospheric conditions such as humidity or aqueous solutions such as seawater, if applicable. As mentioned earlier, there is mounting support for the idea that fretting is a chemical as well as mechanical process. Poon and Hoepnner [15] showed that, of these variables, the chemical elements played a larger role in reducing the fatigue life of a material under fretting fatigue. Conducting experiments on the same material in both ambient air and vacuum conditions, they found that the specimens in the vacuum environment experienced fatigue life spans 10-20 times longer than those

tested in ambient air. However, other experimental results have shown that environmental effects may create certain conditions that aide in alleviating the harmful fretting process. Conner, et al [16] state oxide debris commonly encountered in open-air testing environments, may enter and fill existing cracks, helping to divert energy from the crack tip. In addition, an increase in the amount of oxide debris on the wear surface may create a slip condition between contact surfaces, reducing the coefficient of friction and thus the experienced stresses. It has been demonstrated that when a material is exposed to fretting fatigue, the oxide film on its surface is damaged, reducing the corrosive resistance of the material. As a result, the fatigue strength is degraded and the material becomes more susceptible to wear from fretting mechanisms and environmental corrosion. In a further attempt to understand the effects of environment, Endo and Gato [17] tested fretting fatigue of aluminum and carbon steel in both humid and dry conditions and found that environmental effect was most dependent on material type. The aluminum alloy was found to be quite sensitive to humidity, experiencing accelerated crack initiation and propagation. Waterhouse and Dutta [18] conducted experiments using a 1% NaCl solution to simulate seawater and found that fretting fatigue life was reduced at high alternating stresses but was improved at lower stress regimes as compared to experiments done in dry conditions. Wharton and Waterhouse [19] attempted to explain this phenomenon with the hypothesis that at higher stresses, environmental corrosion increases crack propagation and reduces fatigue life while, at lower stress levels, the protective corrosive debris formed remains in place, acting to retard crack propagation and improve fatigue life. Lietch [20] conducted fretting fatigue tests simulating environmentally corrosive conditions with the use of synthetic seawater. Using un-peened specimens, he found that fretting fatigue life was reduced under low cycle fatigue (high stress) but increased under high cycle fatigue conditions (low stress). These results were consistent with the hypothesis of Wharton and Waterhouse.

2.2 Shot-Peening

2.2.1. Introduction to Shot-Peening

Shot-peening is one of the most effective surface treatment processes against fatigue and is widely used in the aerospace industry. As mentioned, a plastically deformed surface layer is created on the contact surface by the bombardment of high velocity particles called shot which is generally 0.1-1.0 mm in diameter [4], shown in Fig. 2.1. This creates a biaxial residual stress on the shot-peened material which is compressive near the surface and tensile within the material, as shown in Fig. 2.2 [21]. In the process, the surface roughness and grain size of the outermost material are altered. The compressive residual stress created, however, is the most significant factor in improving fretting fatigue life, according to Mutoh, et al [22], and will reach a depth of one-quarter to one-half of the shot diameter [4]. This compressive residual stress can act to close pre-existing cracks and reduce crack propagation. However, if done incorrectly, shot-peening may create a brittle material and have adverse effects on fatigue life. According to Lee [8], in order to optimize fatigue strength, control parameters should be carefully considered, including percentage of surface coverage, shot hardness and shape, velocity, angle of impingement and shot intensity.

2.2.2. Shot-Peening Intensity and Coverage

Shot-peening intensity, specified in terms of the Almen scale, is a measure of shot-peening stream energy. This parameter gives some indication of the magnitude and distribution of the induced residual stress. Shot size and velocity affect the Almen intensity rating. Experiments have been conducted in the past to determine the effects of shot peening intensity on the residual stress profile and fretting fatigue behavior. Using 4, 7 and 10 Almen intensity (4A, 7A, 10A), it was observed that residual stresses on the surface varied little from one Almen intensity to the next. However, beneath the surface peening intensity

showed to have a significant effect on the residual stress profile. Additionally, compressive depth increased with increasing Almen intensity. It was also observed that when undergoing fretting fatigue, crack initiation occurred on the surface of the 4A and 7A peened materials and below the compressive stress depth of the 10A peened material. This was attributed to the greater residual tensile stress created by the 10A peening process [23, 24]. Surface coverage also plays an important role in fretting fatigue strength and is defined as the ration of the peened surface area to the entire specimen surface area. Obviously, no residual compressive stress is created on surface areas that remained unpeened and thus, crack initiation and stress corrosion cannot be curtailed [23]. It is essential to achieve 100% coverage when shot-peening in order for it to be effective against fretting fatigue. Mattson, et al [25] determined, however, that once 100% coverage was achieved, additional bombardment of shot to further improve fatigue life was futile because no increase in residual stress levels was made. An intensity of 7 Almen was used in the current experimentation and compared to results that used various shot-peening intensities.

2.3. Fatigue Parameters

Fatigue parameters typically fall under four main categories, as explained by Lykins [26]. These are: empirical techniques, fracture mechanics techniques, fretting fatigue specific techniques and plain fatigue techniques. These four techniques will be summarized in the sections to follow.

2.3.1. Plain Fatigue Techniques

These techniques are based on the stress and strain histories of the plain fatigue specimen and are used to develop parameters that aid in predicting fatigue life. These techniques are applicable to the case of high cycle fretting fatigue only if the two are related in terms of stress concentration. In other words, stresses experienced at the trailing edge of contact in a fretting configuration must be modeled as stress concentrations, which result

from stress risers such as notches or holes, in a plain fatigue configuration. Another thing to consider is that stresses experienced in the contact region of a body undergoing fretting fatigue are multi-axial, according to Namjoshi, et al [11] Consequently, if a plain fatigue technique is to be applied fretting configuration, it must incorporated multi-axial stress states. Namjoshi proposed numerous multi-axial plain fatigue parameters, all of which fell under one of two categories: equivalent stress models and critical plane models. When using the equivalent stress model, an equivalent cyclic scalar parameter must be developed, often in terms of a mean stress to be used as well as the uniaxial stress vs. fatigue life data. However, when in multi-axial stress configurations, the definition of mean stress is unclear. Therefore, using the equivalent stress model is not always practical. The critical plane model, however, has been found to correlate well with experimental observations. Researchers have observed that fretting fatigue cracks often occur on a particular plane. For that reason, researchers have recently focused on developing parameters applicable to multi-axial, plain fatigue techniques using stresses found on the critical plane [27].

Coffin [28] showed that in the low cycle fatigue regime, fatigue life can be expressed as:

$$\left(\frac{\Delta\varepsilon}{2}\right)_p = \varepsilon_f^{'}(2N_f)^{c'}, \tag{2.1}$$

where $\left(\frac{\Delta\varepsilon}{2}\right)_p$ is known as the plastic strain amplitude, $\varepsilon_f^{'}$ is the fatigue ductility coefficient, N_f is the number of stain reversals to failure (1 reversal = ½ cycle) and c' is the fatigue ductility exponent.

2.3.1. Empirical Techniques

Researchers in the past have attempted to predict failure due to fretting fatigue using empirical formulas. Most authors tried to explain the reduction in life caused by fretting as a function of the alternating applied stress. However, when considering fretting fatigue, it was ignored that a stress concentration is developed at the edge of the contact surface due to the applied normal, tangential and axial loads [5]. Harris [29] developed a sensitivity index for fretting fatigue of Ti-6Al-4V and showed that the most crucial idea in developing this sensitivity parameter was modifying the stress concentration, not the applied normal stress. Hoeppner and Goss [30] studied fretting fatigue to determine at what point damage due to fretting begins and were able to show that fretting contact results in damage after a certain percentage of the fatigue life.

When using such empirical techniques, the authors generally did not try to establish any relationship between the change in applied loading condition and the change in stress along the contact surface. Instead, they focused on showing that fretting reduced plain fatigue life due to parametric variations in certain loading conditions, namely the applied normal stress.

2.3.2. Fracture Mechanics Techniques

As mentioned, there is a stress concentration that develops during fretting fatigue at the edge of the contact due to the applied normal, tangential and axial loads. A stress intensity factor for the highly stressed contact region was developed by Lindley [31], which enabled the loading conditions that would lead to crack growth and arrest behavior to be determined. The techniques of fracture mechanics have their limitations, however. Initially a crack length must be assumed or an estimate of the maximum flaw size tolerable for infinite fretting fatigue life must be given. Previous research shows that crack initiation begins at between 50-90% of fatigue life for high cycle fretting fatigue. Unfortunately, it is difficult to

be more exact than that and impossible to determine the exact fatigue life required developing an initial crack. Because of this it is becoming more difficult to develop any kind of fatigue parameter under high cycle fretting fatigue conditions using fracture mechanics techniques. Furthermore, these techniques do not provide any means by which to predict the remaining fatigue life left; that is the number of cycles for the specimen to fail once an initial crack has been developed. Yet another setback of this practice is that some knowledge of the crack orientation must be possessed [5]. Due to the hindrances of this method, it is felt by some that fracture mechanics is not an appropriate for high cycle fretting fatigue conditions. The fracture mechanics approach may be used to analyze fatigue failure when a large proportion of fatigue life is spent in crack propagation. However, in high cycle fretting fatigue, a large proportion of fatigue life is spent in developing crack nucleation and growth to a detectable size.

2.3.3. Fretting Fatigue Specific Techniques

Some parameters specifically applicable to fretting fatigue were presented by Ruiz, et al [32]. These parameters are defined below:

$$\kappa_1 = (\sigma_T)_{\max}(\tau\delta)_{\max} \tag{2.2}$$

$$\kappa_2 = (\sigma_T \tau\delta)_{\max} \tag{2.3}$$

where $(\sigma_T)_{\max}$ is the maximum tangential stress and $(\tau\delta)_{\max}$ is the maximum frictional work. It was proposed that damage due to fretting fatigue depends on the work done by the frictional force between the fretting surfaces. Equation (2.2) is a measure of the frictional energy expenditure density. The frictional work term $(\tau\delta)$ represents the mechanism that nucleates cracks. It is then opened and propagated by the maximum tangential stress $(\sigma_T)_{\max}$. Equation (2.3) is a modified form of the first equation and asserts that under

fretting fatigue conditions, crack nucleation can also depend on maximum tangential stress. Researchers found that the second parameter (κ_2) agreed with the crack initiation location along the interface but Lykins, et al [33] found these parameters to be inadequate when it comes to predicting crack initiation behavior. In addition, Lykins [16] found no distinct trend between Ruiz's parameters number of fretting fatigue cycles to crack initiation. He also noticed inconsistency regarding the location of crack initiation when compared to his experimental observations.

For this reason, the following parameter was developed by Elkholy [34]:

$$\frac{\sigma_R}{p_0} = 2f\left[1-\exp\left(\frac{-Eu}{ap_0}\right)\right], \tag{2.4}$$

where σ_R represents the fretting fatigue strength reduction, p_0 is the maximum pressure experienced due to the normal load, f is the coefficient of friction, E is Young's Modulus, u is the slip distance and a represents the contact half length. It should be noted that this parameter is only applicable when the same stress ratio is used in fretting fatigue tests. Elkholy, when developing this parameter, recommended subtracting the strength reduction factor from the material's plain fatigue strength. He also found a way to incorporate the slip distance (u) into the parameter.

2.4 Contact Mechanics

In the current study, the fretting fatigue environment will be experimentally simulated using a cylindrical body in contact with a flat body. In this case, fretting pads will be used as the cylindrical bodies and the test specimen will represent the flat body. These two geometries create a contact problem that must be solved. The two bodies in contact, the fretting pad and test specimen, are assumed to have infinite boundaries and the resulting

analytical equations were formulated based on the displacement relationships of the contacting bodies. Figure 2.3 shows the relationship between the contacting bodies in the fretting fatigue configuration. In the diagram, A represents the cross-sectional area of the test specimen, P is the applied contact load, Q is the reacted tangential load, σ_{axial} indicates the applied axial stress, d is the specimen thickness, b is its half thickness and a represents the contact half width. The radius of the fretting pads is a constant, r, and the radius of the fretting specimen is infinite; that is, a flat surface was used.

When two bodies are brought into contact with each other using an applied contact load and placed in a fretting configuration, a stick zone within the contact surface will exist such that the displacement of adjoining points on the fretting pad and specimen will be coincident on the contact surface. In addition, a pressure distribution p(x,y) will be created by the contact load, usually known as the Hertz solution. The determination of this pressure distribution depends upon two assumptions: first, the radii of the contacting bodies are both large compared to the contact dimensions and secondly, the bodies in contact have infinite boundaries. This second assumption is held if the following equation is satisfied: b/a > 10. If this condition is not met, results will deviate significantly from those done using finite element analysis [12]. Furthermore, the contact surfaces are idealized as parabolas, giving a weight function:

$$w(x) = \sqrt{a^2 - x^2}\ , \tag{2.5}$$

where a is the contact half width. Hills and Nowell [1] went on to show the following derivation, beginning with the pressure distribution:

$$p(x) = -\frac{k}{a}\sqrt{a^2 - x^2}\ , \tag{2.6}$$

where k is the radius of curvature,

$$k = \frac{1}{R_1} + \frac{1}{R_2} \tag{2.7}$$

where R_1 and R_2 are the radii of curvature of the fretting pad and test specimen. The following equation then shows the equilibrium relationship between the applied contact load and the pressure distribution:

$$P = -\int_{-a}^{a} P(\xi)d\xi = \frac{\pi k a^2}{2A^*}. \tag{2.8}$$

Using equations (2.6) and (2.8) gives the following equation:

$$p(x) = -p_0\sqrt{1-\left(\frac{x}{a}\right)^2} \tag{2.9}$$

where p_0 is the maximum pressure, or Hertzian Peak Pressure, and is defined as,

$$p_0 = \frac{2P}{\pi a}. \tag{2.10}$$

The contact half width (a) is found from Eqs. (2.7) and (2.8) to be,

$$a = \sqrt{\frac{8PR_1}{\pi}\left(\frac{1-\upsilon^2}{E}\right)}, \tag{2.11}$$

remembering that $R_1 = \infty$ for a flat surface. The axial stress experienced from the applied contact load (P) is given as:

$$\left(\sigma_{xx}\right)_{contact} = -p_0\frac{\sqrt{a^2 - x^2}}{a}. \tag{2.12}$$

Upon applying the contact load (P), there will be a stick zone towards the center of the contact surface and two slip zones on either side of the stick zone as shown in Fig. 2.4. The stick zone is the area where the adjoining contact points of the two bodies move together. In a fretting fatigue configuration, this zone is determined from contact geometry, contact pressure and the coefficient of friction. The formation of this stick zone results in the

remotely applied stresses of high magnitude near the contact surface which leads to premature crack initiation. In the area of the slip zones, however, adjoining contact points on the fretting surfaces move independently of each other.

The distribution of shear stress along the contact surfaces is expressed as:

$$q(x) = \frac{C}{\sqrt{a^2 - x^2}} \tag{2.13}$$

where $C = \frac{Q}{\pi}$. Q is the shear stress along the contact length, obtained from the following equation:

$$Q = \frac{fp_0\pi}{2a}\left(a^2 - c^2\right). \tag{2.14}$$

The stick zone is defined as:

$$\frac{c}{a} = \sqrt{1 - \left|\frac{Q}{fP}\right|}. \tag{2.15}$$

The stress distribution created by the tangential load (Q) in the x-direction is shown as:

$$\left(\sigma_{xx}\right)_{\text{tan}\,gential} = 2\,fp_0 - \frac{2}{\pi}\int_{-a}^{a}\frac{q'(x)}{x+a}dx\,, \tag{2.16}$$

where q'(x) is given as,

$$q'(x) = -\frac{fcp_0}{a}\sqrt{1 - \left(\frac{x-e}{c}\right)^2}\,. \tag{2.17}$$

The expression e in the above equation is expressed as follows:

$$e = \frac{\sigma a}{4\,fp_0}, \tag{2.18}$$

where

$$\sigma = \frac{E\varepsilon_{xx}}{1-\upsilon^2}. \tag{2.19}$$

ε_{xx} is the strain induced by the axial tensile stress $\left(\sigma_{axial}\right)$. The total axial stress experienced between the fretting surfaces, specimen and pad, is given by:

$$\sigma_{xx} = \left(\sigma_{xx}\right)_{contact} + \left(\sigma_{xx}\right)_{\tan gential} + \left(\sigma_{xx}\right)_{axial}. \tag{2.20}$$

Typically, this analytical solution is used to validate results obtained using finite element analysis methods.

2.5. Simplifying the Experimental Procedure

Fretting fatigue has been simulated, studied and analyzed for a number of years and as it has become better understood, an idealized experimental apparatus or testing schematic has been developed. This was done in an effort to isolate certain controlling variables and simplify the analysis. In this general fretting fatigue configuration, shown in Fig. 2.5, the fretting specimen is brought into contact with two cylindrical surfaces. This idealized contact configuration was discussed above. The axial stress $\left(\sigma_{axial}\right)$ is typically applied to one end of the specimen while the other is held fixed. The stress is applied by a hydraulic force actuator which can be controlled to produce the desired magnitude, cycle frequency, waveform and stress ratio, $\frac{\sigma_{\min}}{\sigma_{\max}}$. This applied axial load generally has a sinusoidal waveform. At the same time, a contact load (P) is applied to the cylindrical or spherical fretting pads at an orientation perpendicular to the direction of the axial load to establish fretting. Fretting pads of this geometry are generally sought because the analytic solutions for the stress and displacement distributions created by these geometries are achievable and have been derived. This contact load induces a tangential load (Q) along the contact surfaces

which forces the specimen and pads to move relative to each other in a partial slip condition. The magnitude of this force is determined by measuring the difference between the axial load applied at the bottom of the specimen by the force actuator and the axial load experienced at the top of the specimen, or the fixed end. These quantities were measured by load cells, placed at both ends of the test specimen, capable of measuring the forces encountered. The difference calculated is equal to the sum of the shear loads experienced on each side of the specimen and is typically divided by two to get the shear load created by each pad. A moment on the pads results from the shear developed between pad and specimen and is typically countered by holding the pads in place with relatively large, steel pad holders designed to encompass and secure the pad. This experimental configuration in the end leads to crack initiation and failure caused by fretting fatigue.

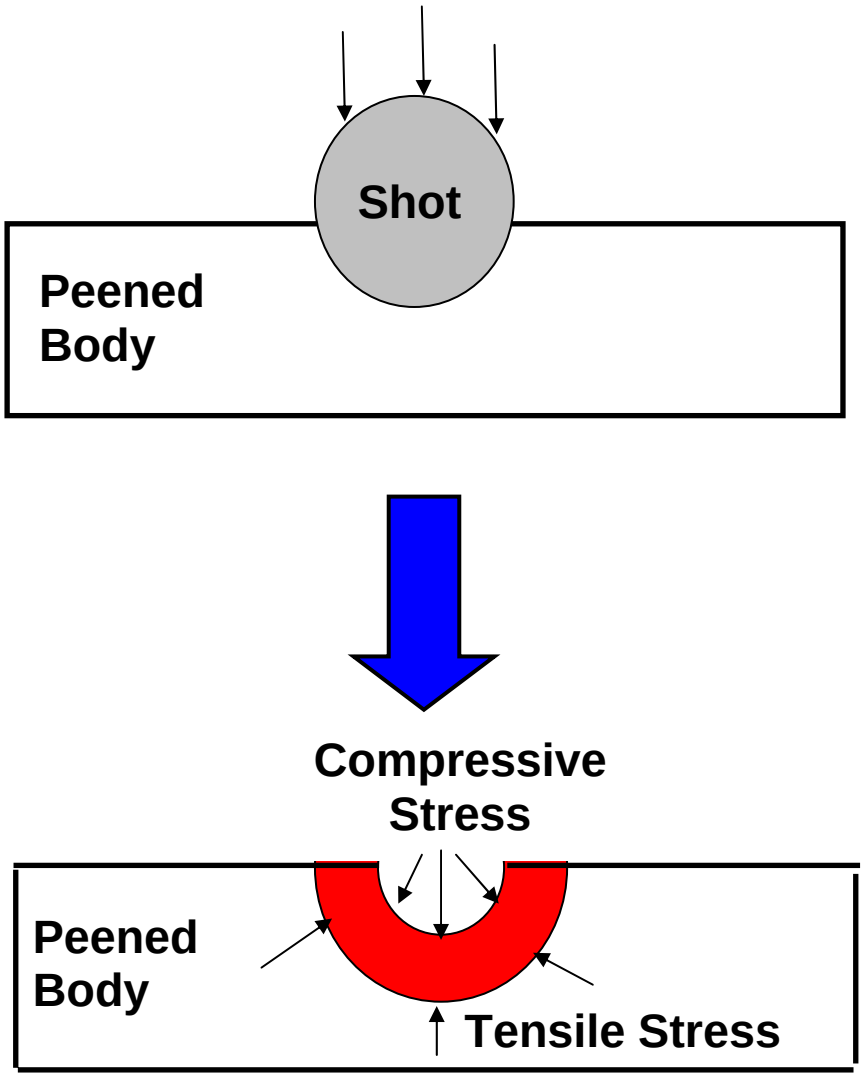

Figure 2.1. Schematic of the shot-peening process and the residual stresses it creates.

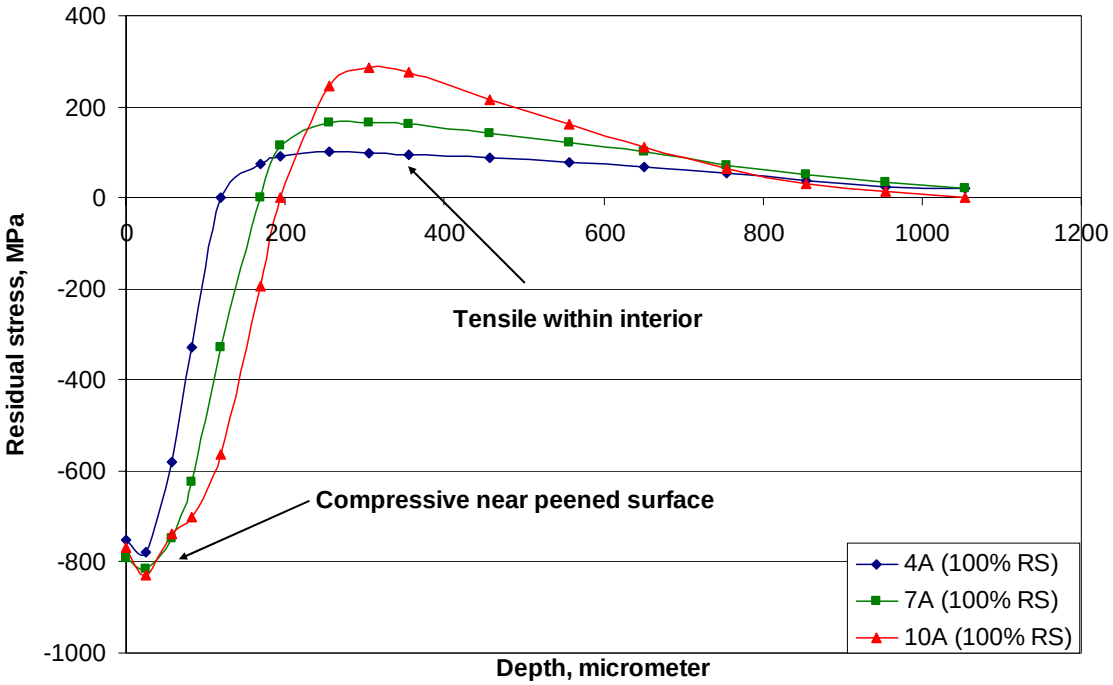

Figure 2.2. Residual stress profiles created by shot-peening at various intensities.

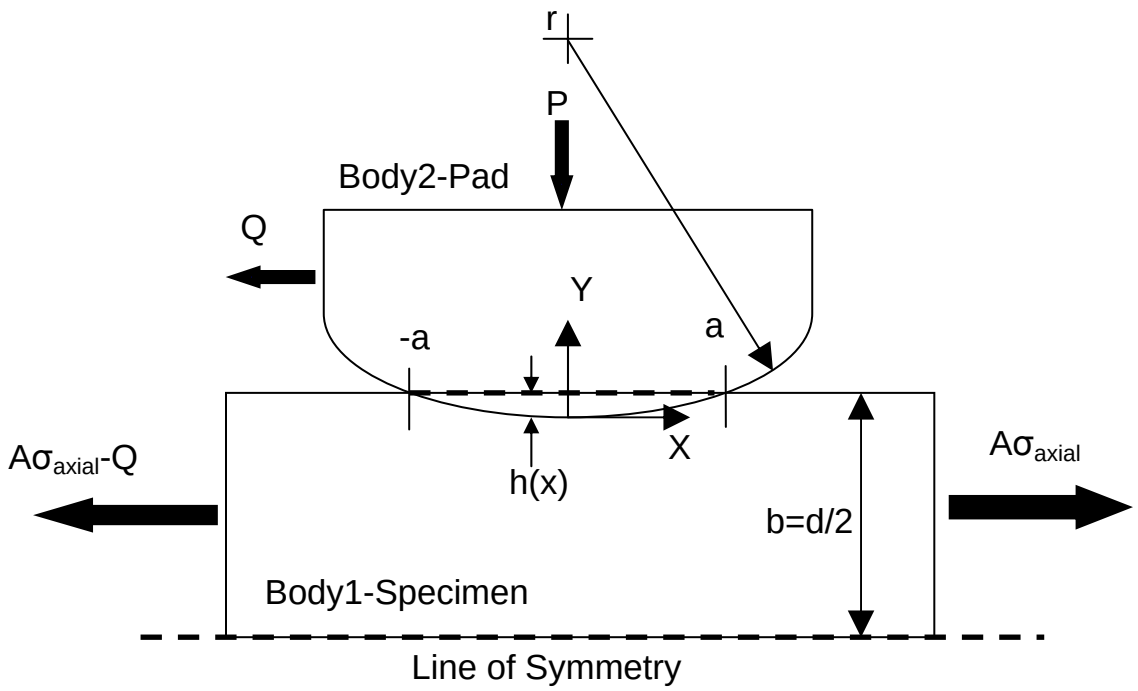

Figure 2.3. Free body diagram of fretting fatigue loads.

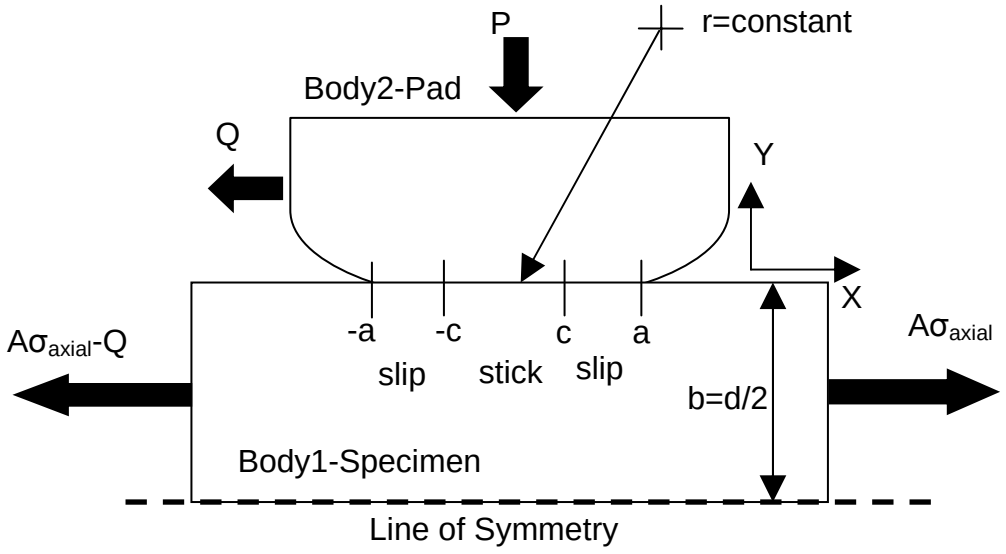

Figure 2.4. Partial slip conditions in fretting fatigue configuration.

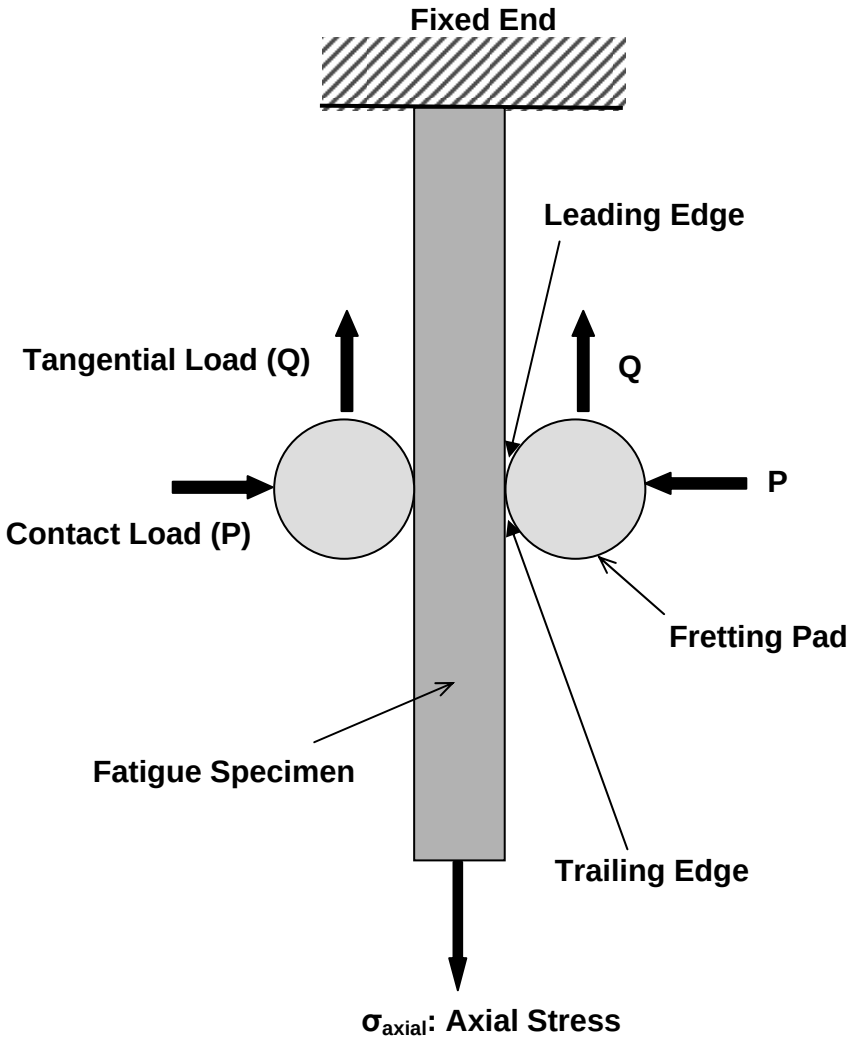

Figure 2.5. Simplified fretting fatigue configuration.

3 Experimentation

Equation Section 3

The purpose of this experimentation was to determine the effects, if any, that polishing a shot-peened specimen might have on the fretting fatigue life of that material, in this case the titanium alloy, Ti-6Al-4V. The hope was that, by removing the textured surface created by the peening process, any defects created that could act as local stress raisers would be removed while the beneficial effects of the residual stress created by peening the specimen still remained, thus improving the fretting fatigue life of the specimen. This chapter discusses the experimental configuration used in this study to investigate the above hypothesis. Specific details of the experimental procedure such as specimen and pad geometry, material properties and load determination are also discussed.

3.1 Experimental Configuration

The fretting fatigue that occurs in turbine engines is a very complex process based on, among other things, geometry and loading conditions. Duplication of this environment for experimental purposes was not feasible due to cost and time restrictions. However, as mentioned in Chapter 2, idealized configurations were used that allowed certain test variables to be isolated and simplified the analysis. Thus, basic geometry and loading configurations were used to determine the effects of shot peening and other surface treatments on high cycle fretting fatigue of Ti-6Al-4V, a material commonly used in turbine engine components. Experiments were carried out using a 22.2 kN servo-hydraulic uniaxial testing machine supplied by MTS, Inc., and were conducted at room temperature in a laboratory environment. This machine, seen in Fig. 3.1, had upper and lower load cells attached to each end of the specimen; the upper load cell was fixed and the lower cell, the actuator, was controlled using

Multi-Purpose Test (MPT) Software capable of controlling the load cell displacement as well as the magnitude, frequency and waveform of the applied load. A schematic of the testing configuration can be seen in Fig. 3.2. In all testing, a tension-tension cyclic loading was applied, meaning that the entire range of stress experienced by the specimen was greater than zero, keeping the part in tension at all times. The fretting process was introduced by bringing the flat specimen into contact with 2 cylindrically surfaced fretting pads, as seen in Fig. 3.3. A constant load (P) was used in all tests, held constant by lateral springs that could be compressed to maintain the desired load and measured by two load cells placed between the springs and fretting fixtures. The fretting fixture used for these experiments was designed and used in the past by former graduate and doctoral students; it was not designed by the MTS Corporation and is not capable of applying the variable contact loads (P) that Jutte [5] used in conducting his experimentation.

3.2 Geometry

Pad and specimen geometries were held constant throughout the testing process and are shown in Fig. 3.4. A standard "dog bone" shaped specimen with a total length (L) of 60 mm was used. The cross-section of the fretting specimen had on average a width (w) of 6.35 mm and a thickness (2b) of 6.35 mm, giving a cross-sectional area (A) of 40.3225 mm^2. After the peening process, the fretting surfaces of the specimens were hand polished to a smooth finish. This process removed approximately $25\mu m$ (0.001 in.) from each fretting surface and reduced the cross-sectional area to 40.0006 mm^2. The peened portion of the specimen can also be seen in Fig. 3.4 as the middle, shaded region. The fretting pad surfaces were not shot-peened. The pads used had widths of 9.525 mm, thicknesses of 9.525 mm and end radii of 50.8 mm.

3.3 Material Properties

The fretting specimens and pads used during this experimentation were both comprised of Ti-6Al-4V, an alloy commonly used in the aerospace industry. The processing techniques used in preparing this material are as follows: The alloy is preheated and solution treated at $935°C$ for one hour and 45 minutes. It is then air cooled and vacuum annealed at $705°C$ for two hours, then cooled again in Argon. The micro-structure this creates shows 60% of α (HCP) phase (platelets) and 40% β (BCC) phase (matrix). The approximate grain size is $10\mu m$. Ti-6Al-4V has the following material properties: a modulus of elasticity, E=126 GPa; yield strength, $\sigma_y = 930MPa$; Poisson's ratio, $\upsilon = 0.3$ and a Brinell hardness of 302 [10]. Shot-peening was applied to the gage section of the fretting specimens only. This peened section can be seen in Fig. 3.3. The surface was peened using ASR-110 cast steel shot using 7Almen (7A) intensity and achieving 100% coverage, as defined by the SAE Aerospace Material Specification (AMS) 2432 standard.

3.4 Applied Load

Axial loads were applied by the MTS 22.2 kN servo-hydraulic uniaxial testing machine, with the maximum stress applied ranging from 500-600 MPa. A stress ratio (R) of 0.1 was used for all experiments. This means that for a maximum applied stress of 600 MPa, the minimum applied stress would be 60 MPa, or 10% of the maximum as indicated by R. Since the entire range of applied cyclic stresses in all tests was greater than zero, the specimens were always in tension, creating a tension-tension condition. The cyclic stress was applied at 10 Hz. A constant contact load (P) of 1335 N (300 lbf) was applied in all tests

and was measured using two load cells in contact with the fretting fixtures on either side of the specimen.

The test machinery also allowed the pressure with which the specimen was gripped to be controlled. In most cases, this grip pressure was set to 8 MPa but in early experiments was set to 12 or even 18 MPa. A number of tests were run to determine at what grip pressure the specimen would begin to slip in the grips. It was originally thought that as high a grip pressure as possible should be used to ensure no slipping. Since the titanium alloy used is a very hard material, there was no danger of crushing the specimen as there might have been with a composite material. Thus, a grip pressure of 18 MPa was used. Eventually, after encountering trouble with the fracture location of the specimen, it was thought that the excess grip pressure might be creating stress risers in the gripping area, causing fracture to occur in this region. It was then determined that the specimen did not begin to slip until a grip pressure of 6 MPa was used. A final grip pressure of 8 MPa was decided upon in an attempt to avoid the development of stress risers while assuring no slip.

3.5 Experimental Procedure

Each test began with a new, shot-peened specimen, a new pair of resurfaced fretting pads and a unique axial stress magnitude. Each pad and specimen was used only once. A stress ratio of R = 0.1 was always used and, with the maximum applied stress, was used to find the effective stress $\left(\sigma_{eff}\right)$ by means of the following equation:

$$\sigma_{eff} = \sigma_{\max}\left(1-R\right)^{m}, \tag{3.1}$$

where m is a material fitting parameter equal to 0.45. As the fretting fixture was a homemade apparatus, meaning that it was not specifically designed and constructed by the manufacturer of the machine, there was an increased likelihood of error when aligning the fretting pads with the specimen. Minimizing this error was the most tedious

portion of the testing procedure. To insure that the fretting pads were as close to orthogonal to the longitudinal axis of the specimen as possible and that contact pressure was applied evenly across the entire width of the specimen, an iterative procedure was used until suitable alignment was achieved. Fretting pads were place into their grooved tracks and clamped down with heavy steel plates containing similar tracks to secure them in place. Approximately 0.25 in. of the fretting pad was placed into the open channel of the fretting fixture to allow contact with only the specimen. The tracks that were machined into the fretting fixture and mating clamping plates were made larger than the pads and permitted some lateral movement of the pads, enough so that significant error in test results could occur if proper care was not taken. To insure pads were aligned with test specimen, pressure sensitive tape was place onto the two fretting surfaces of the specimen. Once the pads were clamped into place, the specimen was placed into the machine and secured by the upper and lower grips. Afterward, the fretting pads were brought into contact with the specimen and the 1335 N contact load was applied. Once this was achieved, the contact load was removed and the test specimen released from the machine. The discolored marks left on the pressure tape by the contact load were then examined. A red mark of equal width that extended across the entire fretting surface of the specimen was ideal, but rarely achieved on the first attempt. Red marks on the pressure tape of varying width or marks that did not extend across the width of the specimen indicated that the pads were not perpendicular to the specimen surface. From there, aluminum shims varying in thickness from 0.001-0.005 in., were placed between the pads and the side walls of the tracks. Shims were placed on one side of the pad or the other, depending on the direction of misalignment and the whole process was repeated.

This was done until pressure marks on the tape were of equal width and extended the width of the specimen on both fretting surfaces.

Once pad alignment was complete, the specimen was removed. At that point it was necessary to warm up the machine. This was done by programming the MPT software to cycle the force actuator up and down at a very low cycle frequency for a very short distance, typically 1 Hz and 0.1 in., respectively. This was done for a minimum of thirty minutes. After warm up was completed, it was time to set up and run an experiment. The upper and lower grips were positioned as close as possible to the fretting fixture to allow as much of the specimen to be gripped as possible. The contact surfaces of the specimen and pads were cleaned with alcohol and, with the pressure tape removed, the specimen was reinserted into grips of the machine. Again, the 1335 N contact load was applied. The MPT software was set to run five million cycles at a constant cyclic frequency of 10 Hz. To begin cycling, the axial load was increased from zero to half of the maximum load over a period of five seconds to avoid any mishaps that might occur from applying a maximum load instantaneously. Once this was achieved, the cyclic loading commenced. Data was collected in a logarithmic pattern with twenty data points taken every cycle, or every 0.05 seconds of a recording cycle. For every data point, the following measurements were taken: time, axial load of the force actuator (lower grip), axial load of the frame (upper grip) and displacement of the force actuator. In addition, the minimum and maximum axial loads experienced by the actuator and frame during the two cycle collection were recorded. Finally, a collection buffer was implemented that recorded and stored the last 500 cycles. This buffer collection continually updated so that when the specimen fractured, loads and displacements

experienced leading up to fracture were recorded, even if the test was running at a point that fell between data collections.

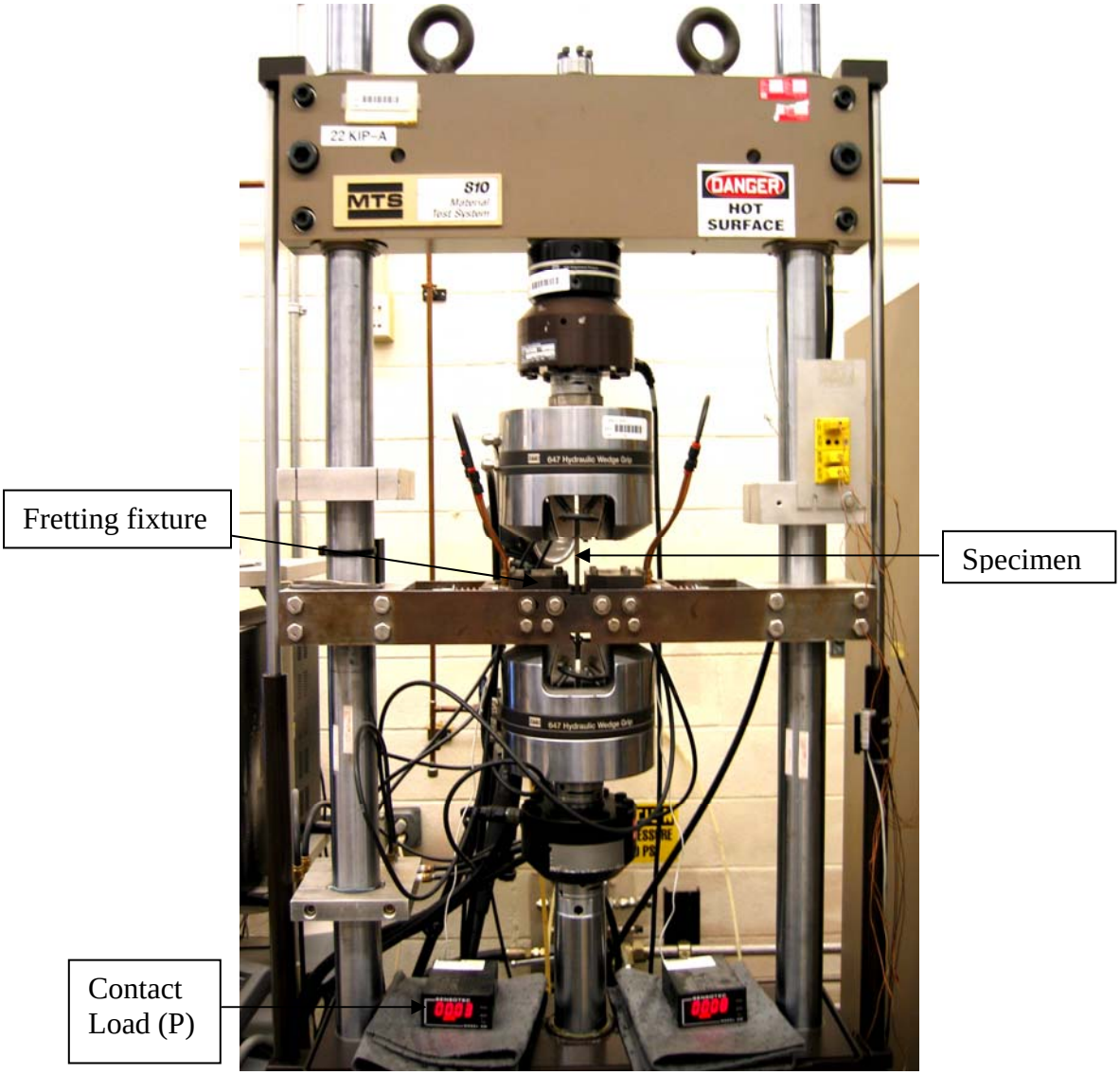

Figure 3.1. MTS 22.2 kN servo-hydraulic, uniaxial testing machine with fretting fixture.

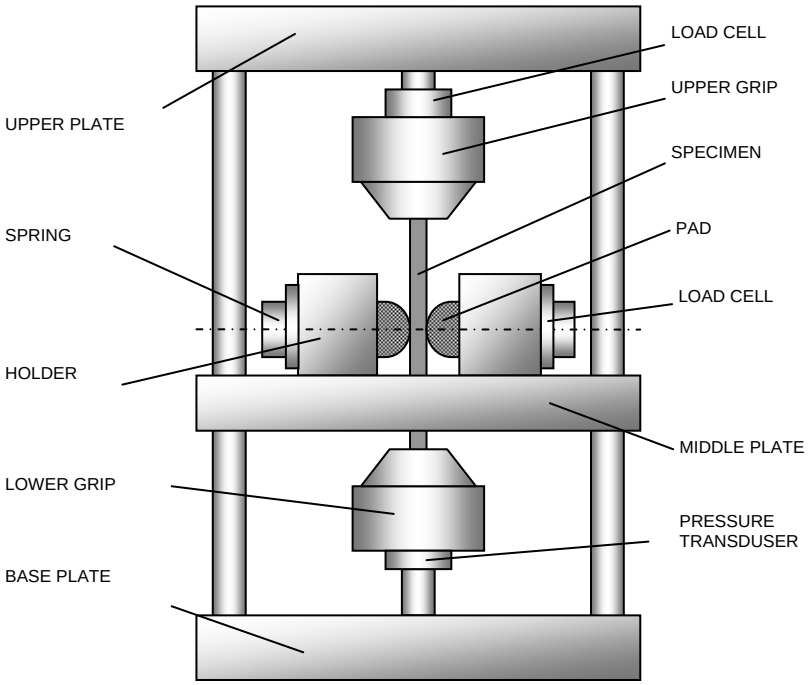

Figure 3.2. Schematic of servo-hydraulic, uniaxial testing machine and fretting configuration.

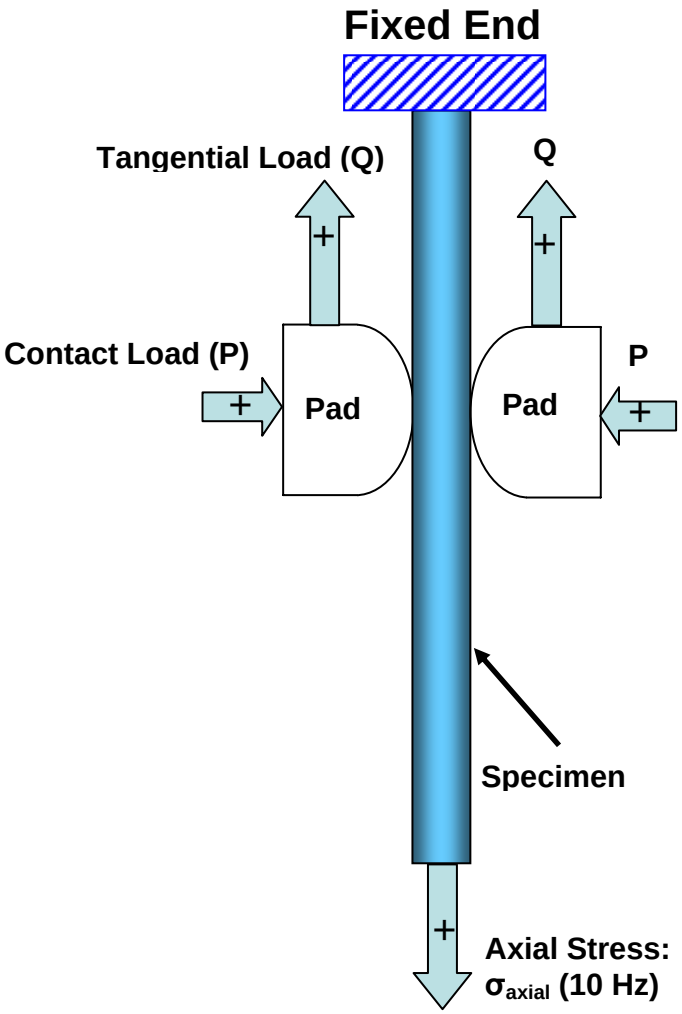

Figure 3.3. Pad and specimen orientation.

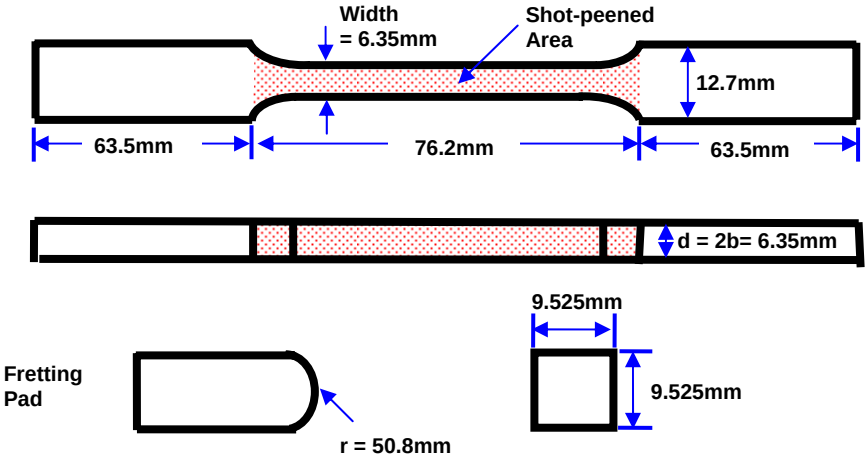

Figure 3.4. Geometries of fretting fatigue specimens and pads.

4 Results & Discussion

Equation Section 4

Seven experiments were conducted in an attempt to determine the effects of polishing the fretting surfaces of shot-peened specimens on fretting fatigue life. Two of the seven were left unpolished and all results were later compared to the results of similar experiments done in previous research. This section discusses the analysis conducted on the experimental results. First, the polishing process was examined and analyzed. It was then determined whether the fretting fatigue condition was met. In addition, tangential load characteristics and fatigue life were examined. The contact area was determined and compared with analytical results determined in Chapter two. These topics are all addressed. Finally, some experimental problems and troubleshooting are discussed.

4.1 Polished Specimens

As stated above, approximately $25\mu m$ thickness was removed from the contact surfaces of the peened specimens by hand polishing them to a smooth finish. This difference is visually compared in Fig 4.1. Looking at Fig. 2.2, it can be seen that removing 25 microns from the fretting surface will have little impact on the residual stresses induced by the shot-peening process. Surface roughness measurements were then calculated and plotted using a profilometer from Taylor/Hobson. These plots over 20 mm lengths of each specimen can be seen in Fig. 4.2 and 4.3. Notice the difference in magnitude of the y-axis scales. The unpolished specimen's roughness varies from the mean value by as much as $4\mu m$ while the polished specimen varies from its mean value

by less than $0.6\mu m$. The root surface roughness values were calculated using the following formulas:

$$R_a = \frac{l}{lr}\int_0^{lr} |z(x)| dx \tag{4.1}$$

$$R_q = \sqrt{\frac{l}{lr}\int_0^{lr} z^2(x) dx}\,, \tag{4.2}$$

where R_a is the universally recognized, most used international parameter of roughness. It is defined as the arithmetic mean of the absolute departures of the roughness profile from the mean line. R_q is the root mean squared (RMS) parameter corresponding to R_a and is sometimes simply referred to as the RMS. R_a and R_q values for the unpolished specimen were determined to be $0.8011\mu m$ and $1.0953\mu m$, respectively, whereas for the polished specimen R_a and R_q were measured to be $0.0570\mu m$ and $0.0776\mu m$, respectively.

4.2 Fretting Fatigue Condition

The first thing done with the experimental data was determine whether or not the required fretting fatigue conditions were met. In order to do this it is helpful to look at a hysteresis plot comparing the axial load and the tangential load, as in Figures 4.4a and 4.5a, which compare polished and unpolished specimens tested at the same σ_{max}. Unless otherwise stated, the term 'axial load' refers to the load measured by the lower load cell connected to the force actuator. In Figures 4.4a and 4.5a it can easily be seen that the minimum and maximum tangential loads (Q_{min} and Q_{max}) stabilize after a short number of

cycles. This is seen in the tight elliptical plots that are achieved after only one hundred cycles and indicates that the partial slip condition has been met. However, it can easily be seen that this occurs more quickly in the case of the polished specimen, as soon as ten cycles. This can be attributed to the fact that the gross slip condition characteristic of early cycles is more quickly reduced because of the greater contact area created by the meeting of two smooth surfaces. During a gross slip condition, the tangential load will reach some maximum and become constant over a portion of the axial load interval. This results in a plot similar to those of the very early cycles of the test, N = 3 and N=5 of the plot in Fig 4.5a. When in a partial slip condition, the tangential load will vary constantly with the axial load. It is important to note that there is no difference in the minimum and maximum tangential load values experienced by the polished and unpolished specimens. Q/P as it varies with axial load is also plotted, where Q/P is an indication of the surface roughness or friction. The behavior of the tangential load (Q) can better be seen by plotting the maximum and minimum tangential loads versus the number of fatigue cycles, as was done in Fig. 4.4c and 4.5c. Notice that Q_{max} and Q_{min} became relatively constant after a short time; this is another characteristic that indicates that the partial slip condition has been met. However, this value reached steady state sooner for the polished specimen than with the unpolished specimen, for the same reason mentioned above. Additionally, there is no difference in the polished and unpolished specimens in terms of the minimum and maximum Q values measured. Maximum and minimum Q/P values are also plotted compared to the number of cycles, Figures 4.4d and 4.5d. It was originally thought that the polished surface would have at least some effect on the tangential loads experienced. To further prove that this is not the case, Figure 4.6 shows a number of data points that

compare $\Delta\sigma$ and Q; including test results from the research of both Albinali and Yuksel. As one can see, the polished surface creates no significant difference in the tangential load induced.

Figures 4.7 and 4.8 show the fretting scars on the specimen and pad, respectively, as well as the corresponding regions of stick and slip. The surface roughness of these scars was measured using the same procedure utilized to measure the roughnesses of the polished and unpolished surfaces before fretting. As was shown, the surface roughness measurements taken before fretting varied significantly between polished and unpolished specimens. The surface roughness plots for both specimens after fretting are shown in Figures 4.9 and 4.10. The first thing of interest to note is that, when comparing the surface roughness measurements of the unpolished specimen for the cases before and after fretting occurred, there is no significant difference. These values are quite comparable. Also of interest is the comparison of surface roughness measurements taken after fretting of the polished and unpolished specimens. These values too are essentially the same. This indicates that, regardless of the original finish of the fretting surfaces, extensive fretting will create a surface roughness that is essentially independent of the initial condition. This suggests that polishing may be inconsequential, considering that the textured surface removed by the polishing will be reapplied by the fretting condition, along with any and all potential for the formation of high stress concentration.

Additionally, the contact load, the axial load and the corresponding tangential load that is experienced are all plotted as they vary with time, shown in Fig. 4.11 over two cycles. This diagram is helpful in demonstrating the interactions between axial, tangential and contact loads. Lee [12] showed that the tangential load varies sinusoidally

and with the same cyclic frequency as that of the axial load. Moreover, he showed that these two loads were always in phase. His findings are confirmed by Fig. 4.11. Although in the current study the contact load was held constant, Lee's research showed that varying this parameter affects the magnitudes of the tangential load measured but has no effect on the waveform, phase lag or frequency of the tangential load.

4.3 Contact Mechanics

Below, a quick analysis was done to compare the experimental contact half width (a) to the analytical solution determined using the theory developed in Chapter 2. Using the results from test number two, the contact width (2a) was measured to be 1.2 mm, shown in Fig.4.12. Eq. (2.11), repeated below for convenience as Eq. (4.3), was used

$$a = \sqrt{\frac{8PR_1}{\pi}\left(\frac{1-\upsilon^2}{E}\right)} \tag{4.3}$$

to determine the analytical solution. Using the material properties for Ti-6Al-4V defined in section 3.3 and a contact radius of 50.8 mm, the analytical contact width (2a) was found to be 0.88 mm. The experimental value was 36% larger than anticipated. This has been a problem in the past for both Lykins and Yuksel when using the same pad geometry. Lykins explained that this phenomenon occurred because of changes in the compliance that took place when the crack size increased, which subsequently resulted in larger contact widths than expected. For shot-peened specimens, the larger contact widths may be attributed to the increased coefficient of friction caused by the additional texture created.

4.4 Fatigue Life

To determine fatigue life trends, the fatigue life in number of cycles was determined and the effective stress $\left(\sigma_{eff}\right)$ calculated using Eq. (3.1). These two values along with the trend line were plotted against each other in an S-N curve, shown in Fig. 4.14. This data was plotted with the results obtained from Yuksel's research. Figure 4.13 shows the S-N curves obtained from Albinali's research for both peened and un-peened specimens at room temperature for comparison's sake. Tables 4.2 and 4.3 show exact values for the data plotted in the figures. It should be noted that, when undergoing testing, problems were encountered that caused fracture on the gripping sections of the specimens in many cases, which will be discussed further in the following section. For this reason it is believed that, in many cases, the fretting fatigue life would be increased. This is what is indicated by the arrows present in Fig. 4.14. The data points without arrows are the ones that fractured due to fretting fatigue. The current data falls within the scatter band created by Yuksel's results. It is apparent that, when compared to Yuksel's data, hand polishing the fretting fatigue specimens does little to prolong the specimen life.

4.5 Residual Stress

Residual stress measurements were taken on the surface of both polished and unpolished surfaces as well as the fretting surface and compared to the typical residual stress profile shown previously to ensure that the specimen was behaving as previous research indicated that it should. The residual stresses measured are shown in Figure 4.15. Averages of a number of values were taken for each measurement and the variation

in measurements is indicated by the error bars. When comparing the bar graph with a residual stress profile, a couple of things indicate that the two graphs are in agreement. First, notice that slightly under the surface of the material the residual stress tends to increase in magnitude. The measurements taken on the polished surface are equivalent to measurements taken just under the surface of the shot-peened material, considering that the polishing removed material from the surface to a depth of approximately 25 microns. Thus, the residual stress measured on the polished surface should be slightly higher in magnitude and this in fact is the case. Secondly, it is known that fretting fatigue causes unavoidable stress relaxation, meaning the some or all of the residual stress created by shot-peening is removed. Accordingly, the residual stress measurements taken on the fretting scar should be noticeably less than those on either the polished or unpolished surfaces. This too is the case, as shown by the bar graph in Figure 4.15.

4.6 Troubleshooting

As mentioned above, some unexpected difficulty was encountered during the testing procedure. Many specimens were not failing at the contact location, the location that fretting fatigue was occurring. Specimens repeatedly fractured on the gripping section of the specimen, shown in Fig. 4.13. The location of the fracture, it should be noted, was consistently at the edge of the grip plate. Various remedies were attempted throughout the testing phase. Initially it was thought that the specimen could be gripped with the maximum grip pressure capable of being produced by the MTS machine, which was 20 MPa. Then, considering that this may cause unnecessary stress risers at the area of contact between the specimen and grip plate, various short trial-and-error tests were run to determine what the minimum grip pressure that could be used without the

specimen slipping was. These tests were similar to the regular testing methods with exception of the fretting fatigue simulation, which was removed. Specimens were subject to the maximum cyclic axial stress that would be encountered during the standard testing for a period of 30 minutes. For each test the grip pressure was reduced by 2 MPa until a grip pressure of 6 MPa was achieved. At this point the specimen began to slip slightly at the initial application of force. For this reason, the grip pressure was set at 8 MPa. This was the value used for the remainder of the experimentation. However, upon running the next test, results were the same. A shot-peened but unpolished specimen was then used and the experimental procedure repeated to determine if something was being drastically affected during the polishing process. The results were the same; fracture occurred on the gripping section, not the gage section. At this point, the alignment of the machine was examined thoroughly. The adjustable tabs used to align the specimen vertically were examined and realigned. Following that, the grips were realigned with a computer aided procedure to ensure that the axial force was being applied exactly along the axis of symmetry of the specimen. The alignment process was to no avail. The next step was to examine the gripping pads themselves. They were switched, meaning that the lower grips were removed and placed into the upper cell and vice versa. Again, this did not correct the problem. Finally, the grips were removed and sent to the manufacturer to be resurfaced. The seventh experiment was run using the newly surfaced gripping pads and gave the best results. The fretting fatigue condition was quickly established and fracture occurred on the fretting surface after 2.99e5 cycles.

The cause of this phenomenon is still uncertain. Upon examining the results of the experiments, even though the specimen was not fracturing in the anticipated location,

the fretting fatigue conditions were met very quickly, showing plots very similar in shape to those of Fig. 4.5 and Fig. 4.6. Notice in Fig. 4.13 the difference in texture on either side of the fracture. The rough or damaged texture on the right was created by the gripping pad and smooth, shiny surface on the right was open to the air and was not part of the gripping surface. This indicates that the specimen fractured at the edge created between where the specimen was gripped and where it was free to the open air. This was a constant occurrence when fracture occurred in the gripping section of the specimen, strongly suggesting that the gripping mechanisms were creating some adverse effect.

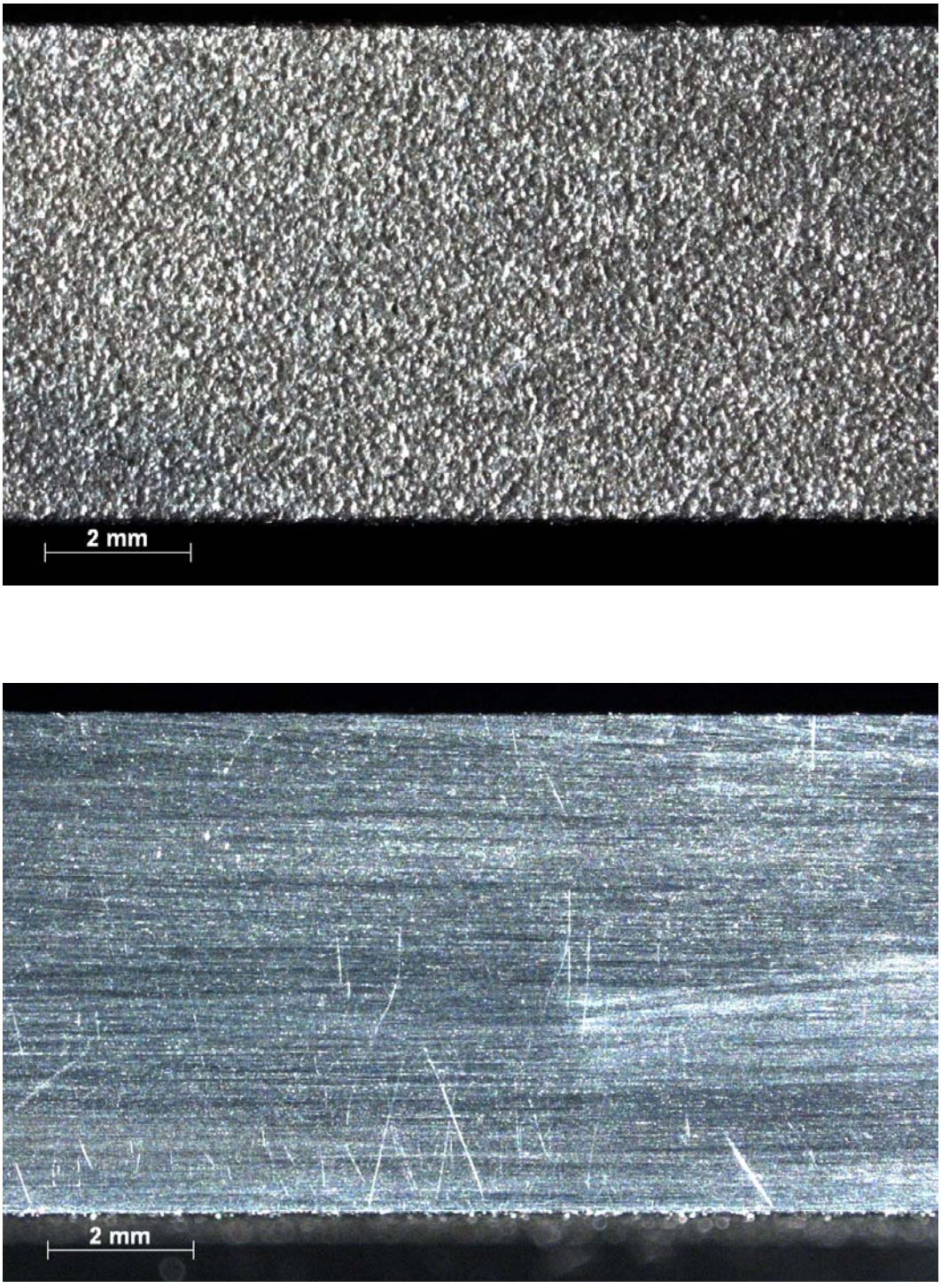

Figure 4.1. Unpolished (top) and polished (bottom) fretting fatigue surfaces.

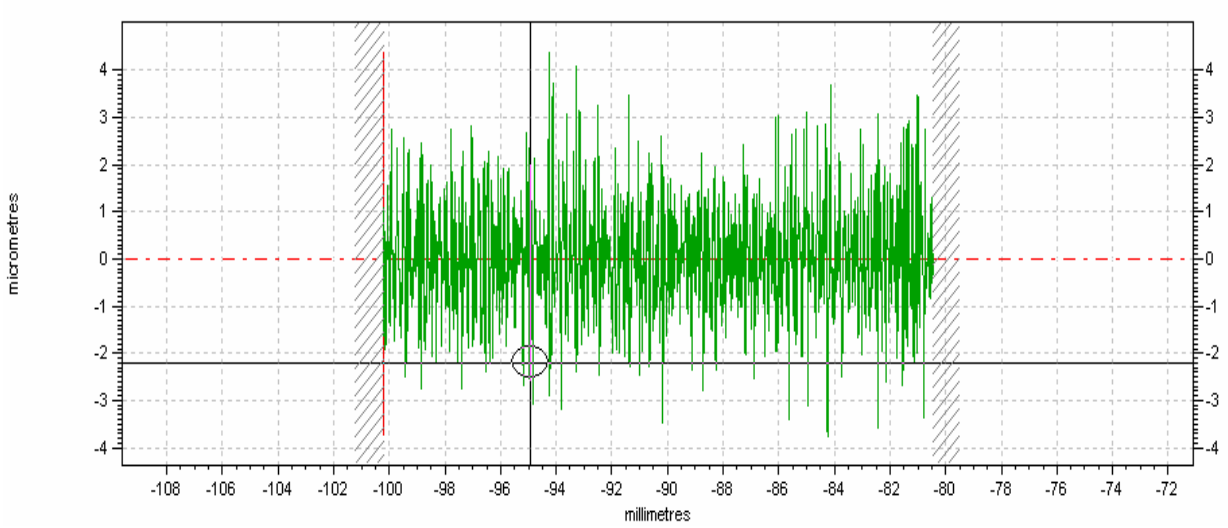

Figure 4.2. Surface roughness of unpolished specimen.

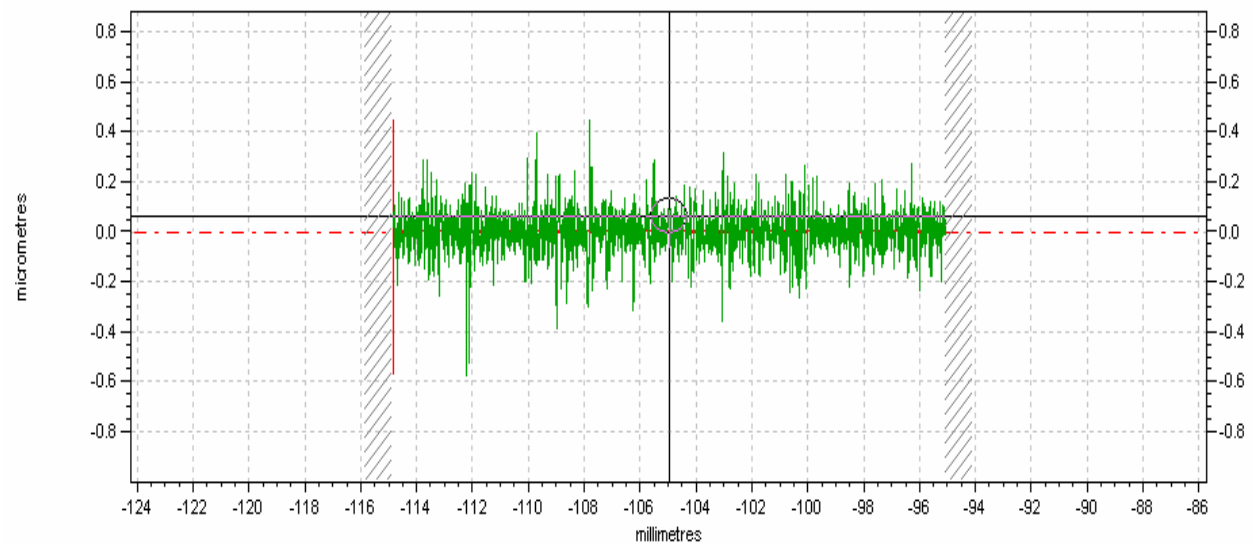

Figure 4.3. Surface roughness of polished specimen.

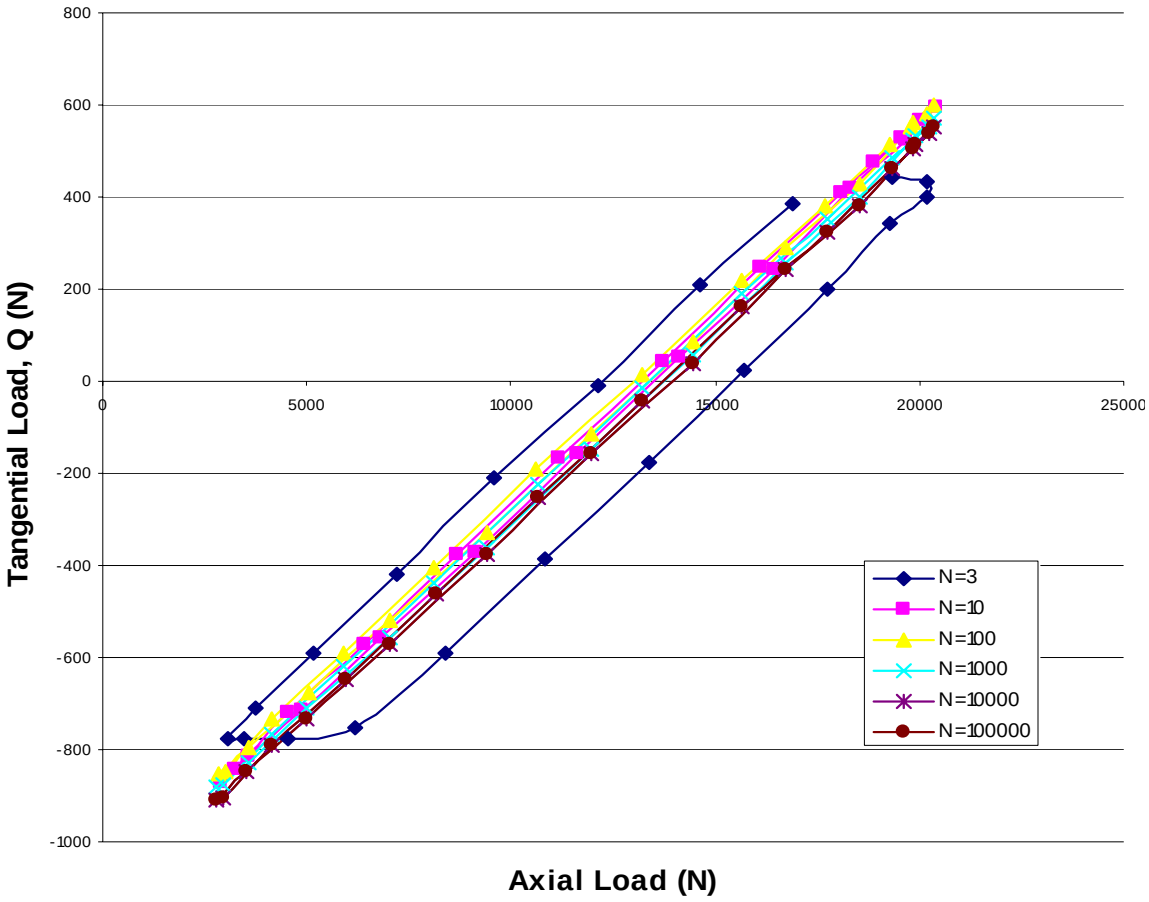

Figure 4.4a. Hysteresis loop for a polished specimen.

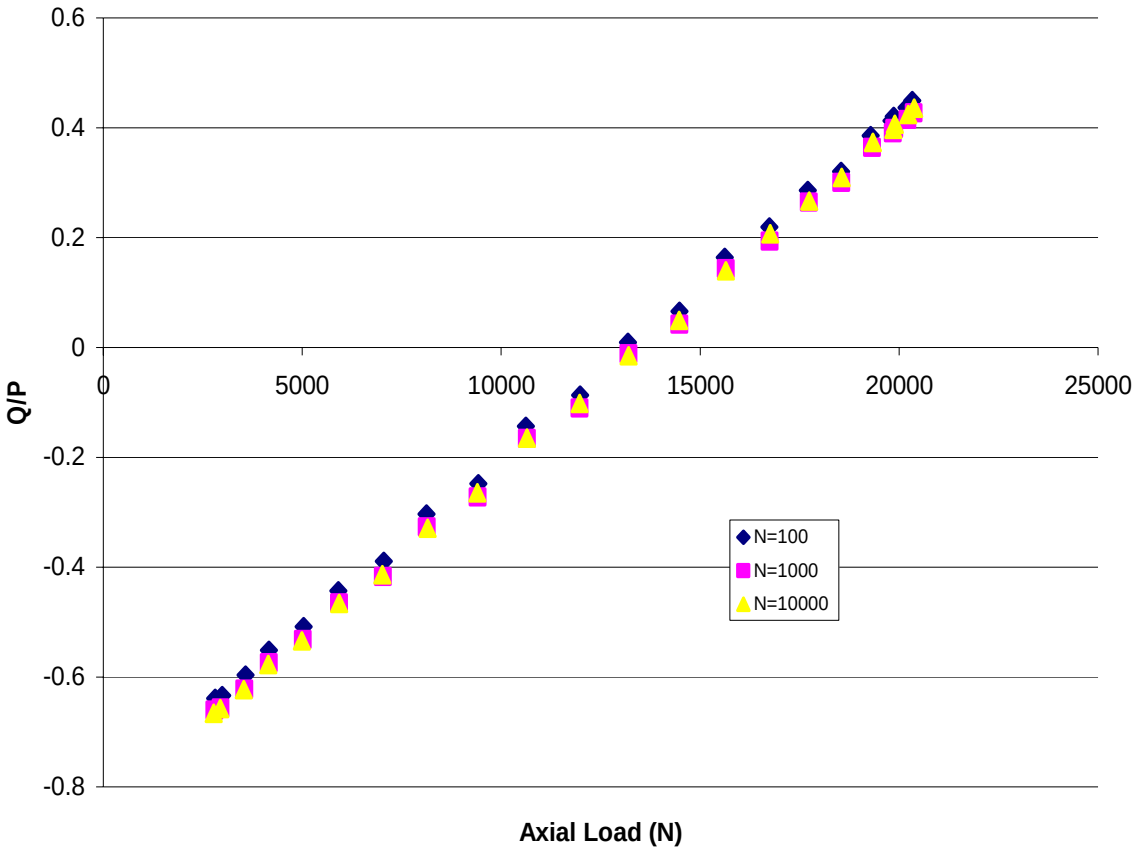

Figure 4.4b. Hysteresis loop comparing axial load and Q/P ratio for a polished specimen.

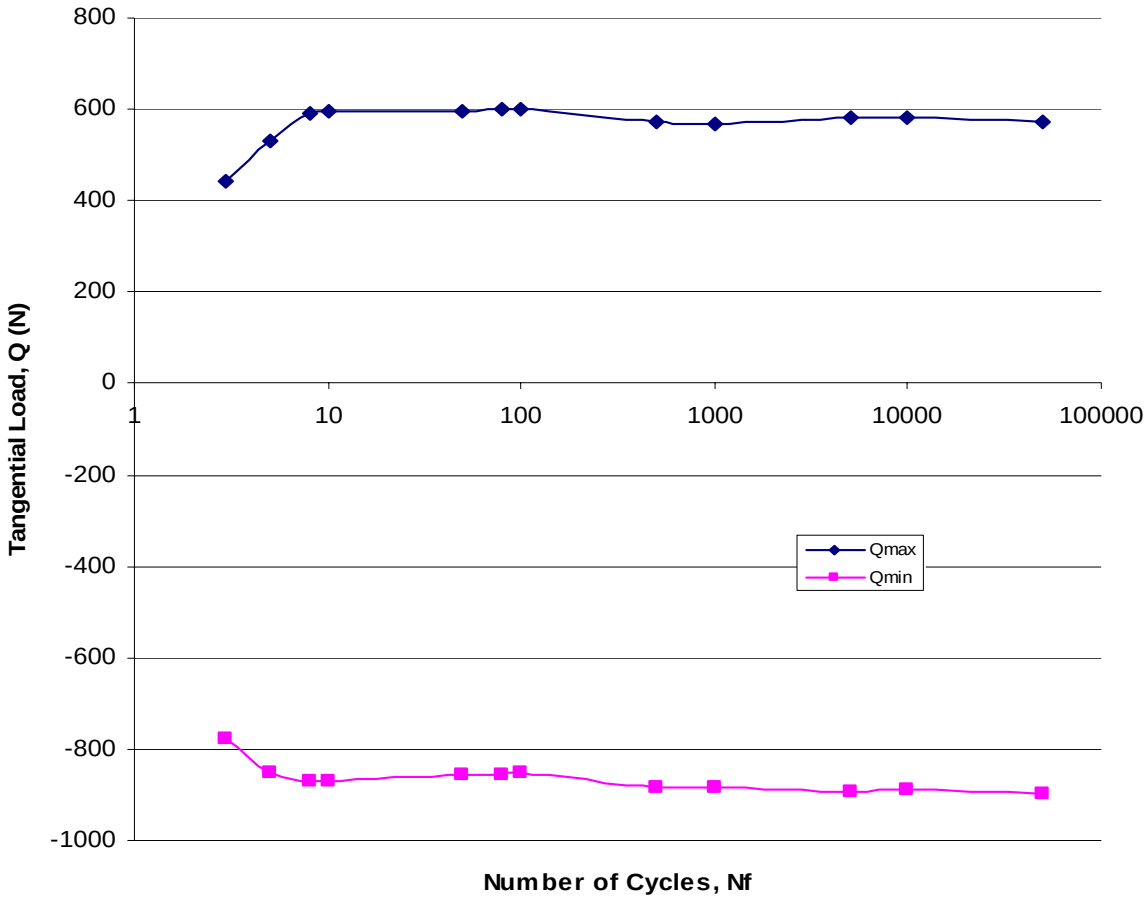

Figure 4.4c. Tangential load vs. fatigue life for a polished specimen.

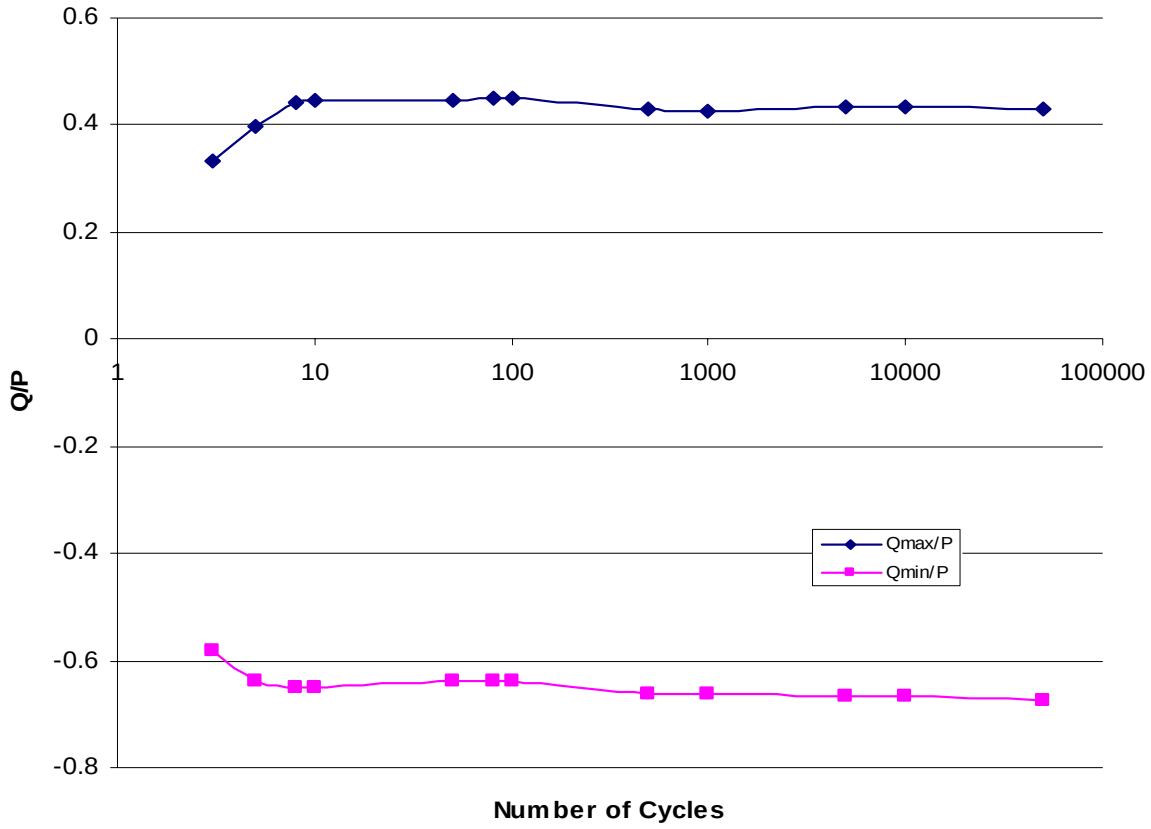

Figure 4.4d. Q/P vs. Number of cycles for a polished specimen.

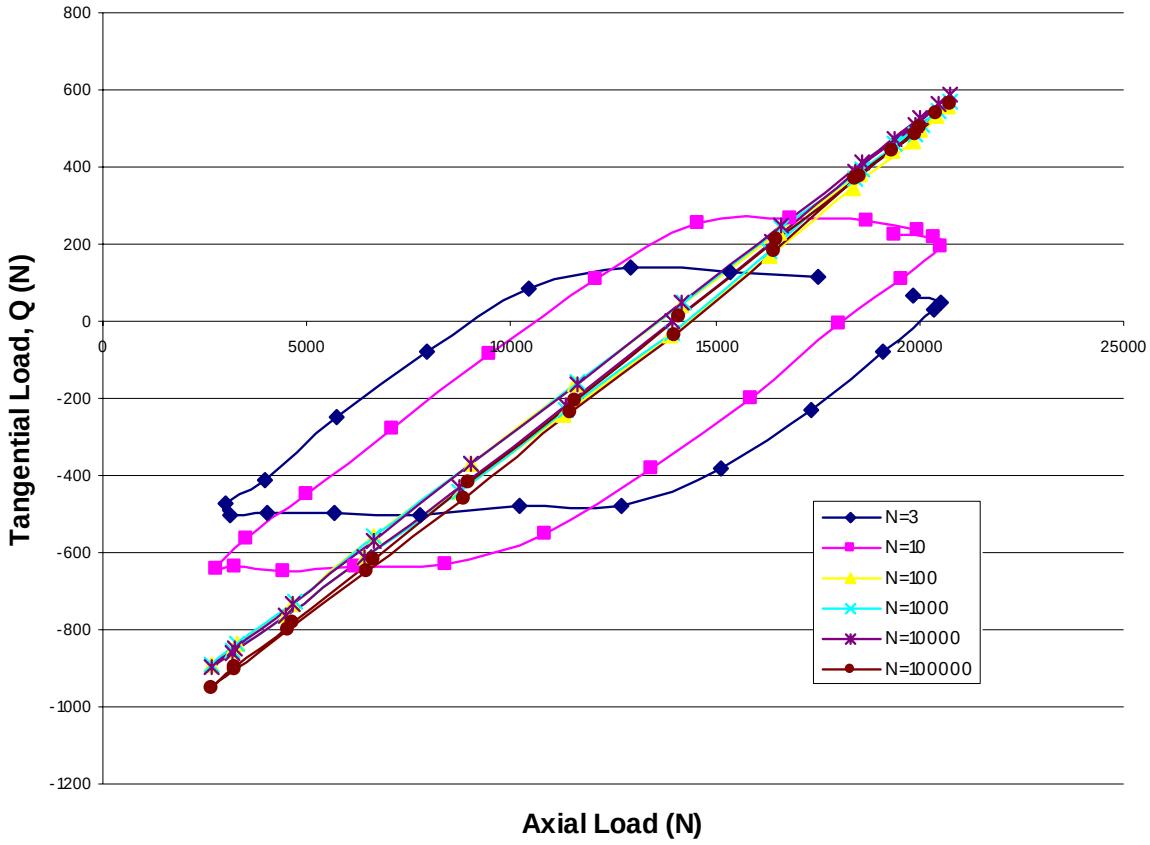

Figure 4.5a. Hysteresis loop for an unpolished specimen.

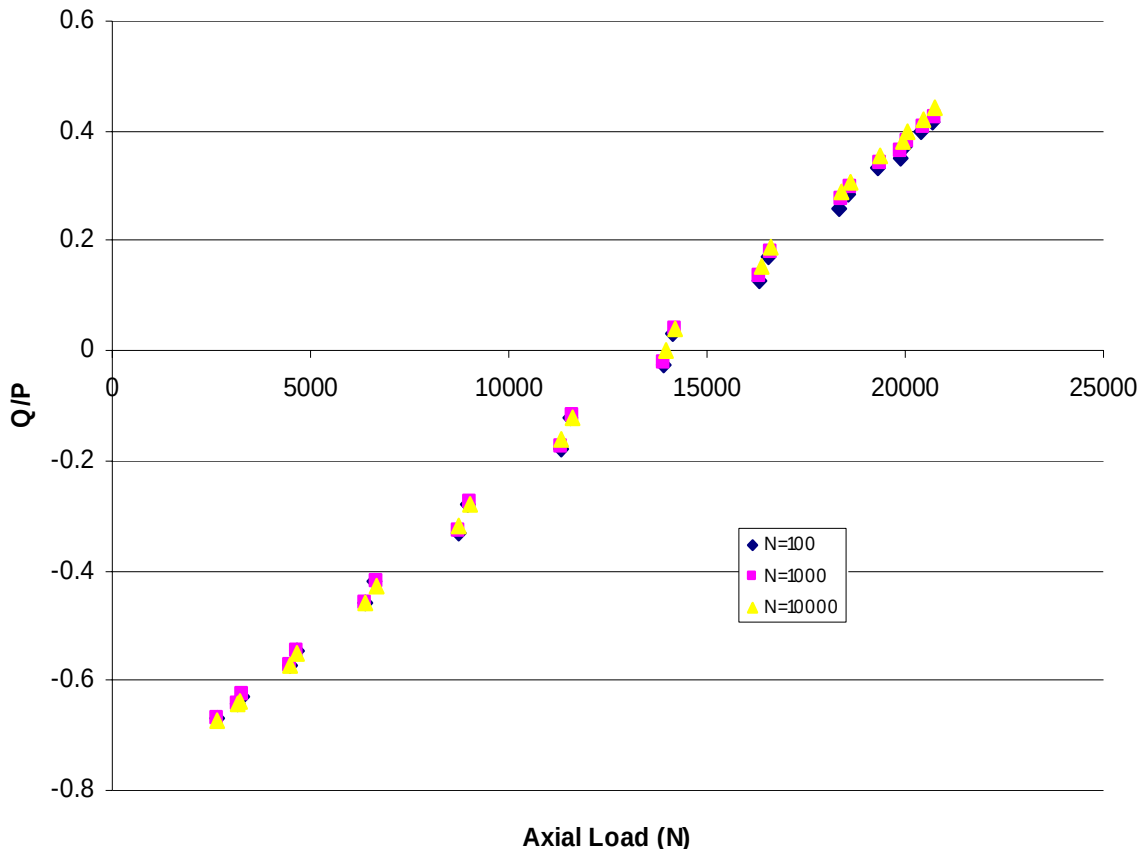

Figure 4.5b. Hysteresis loop comparing axial load and Q/P ratio for an unpolished specimen.

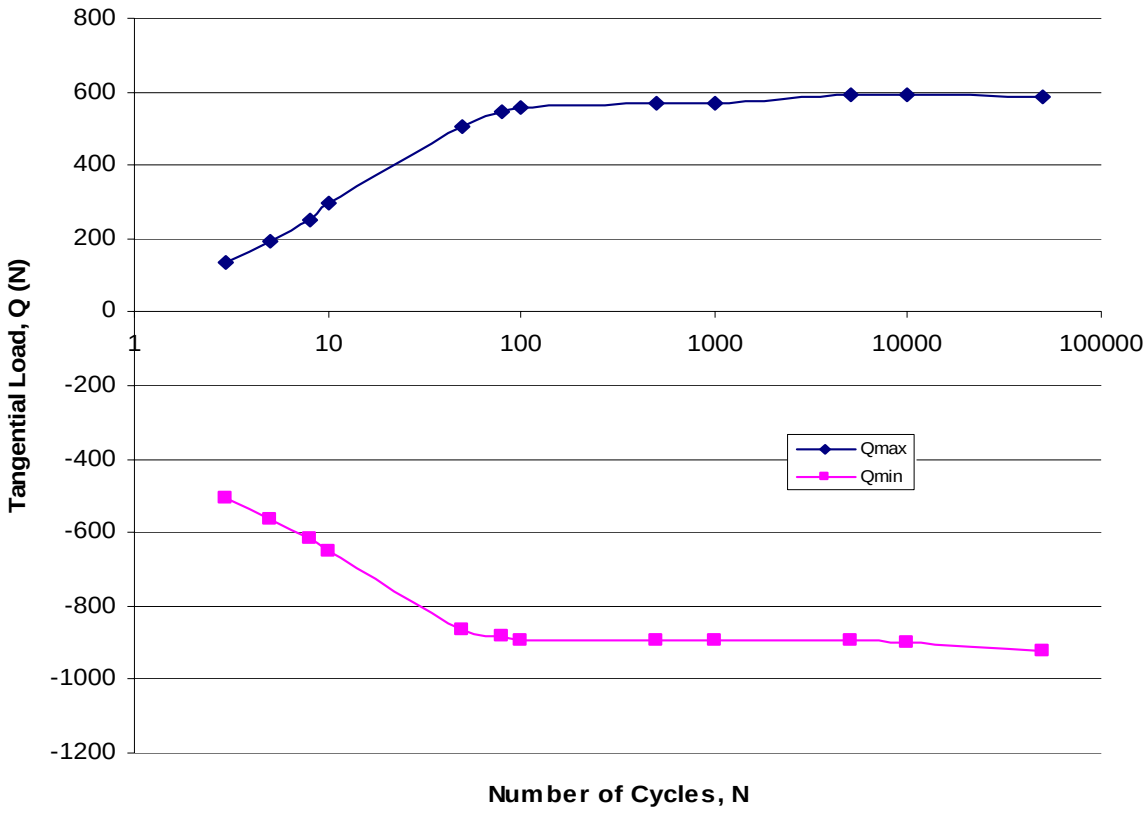

Figure 4.5c. Tangential load vs. fatigue life for unpolished specimen.

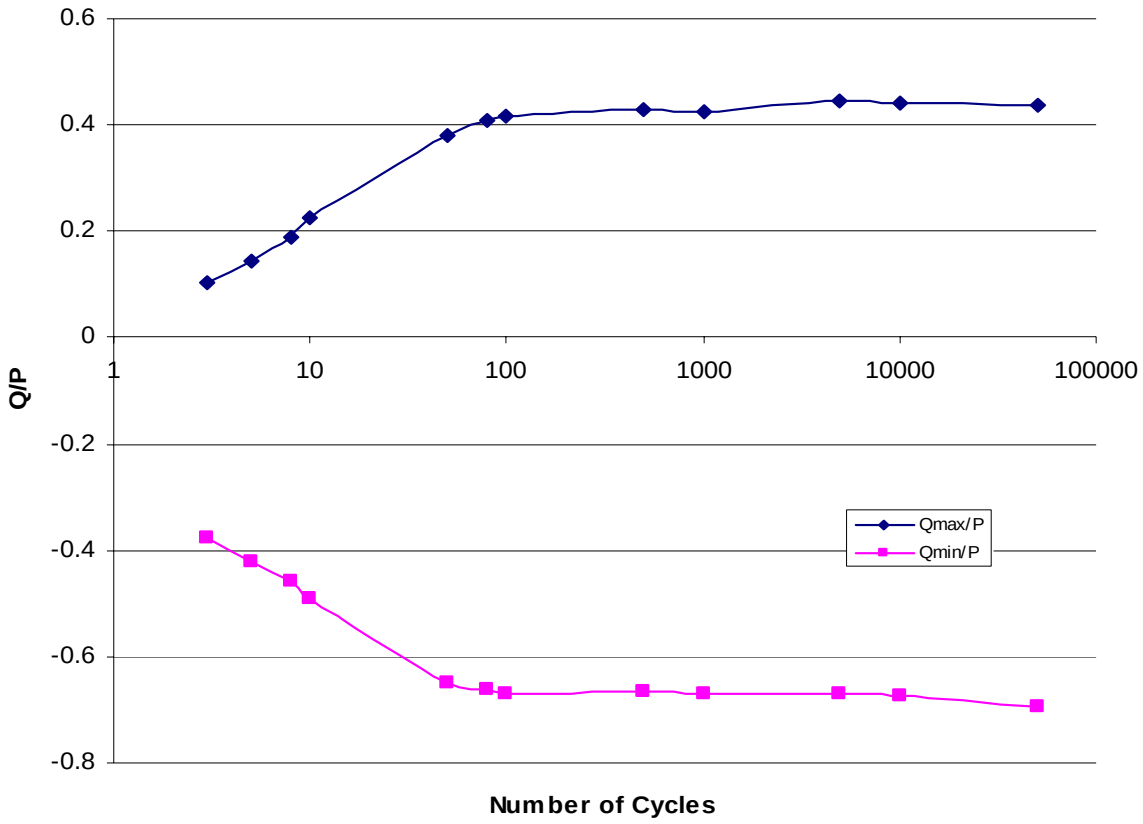

Figure 4.5d. Q/P vs. Number of cycles for a unpolished specimen.

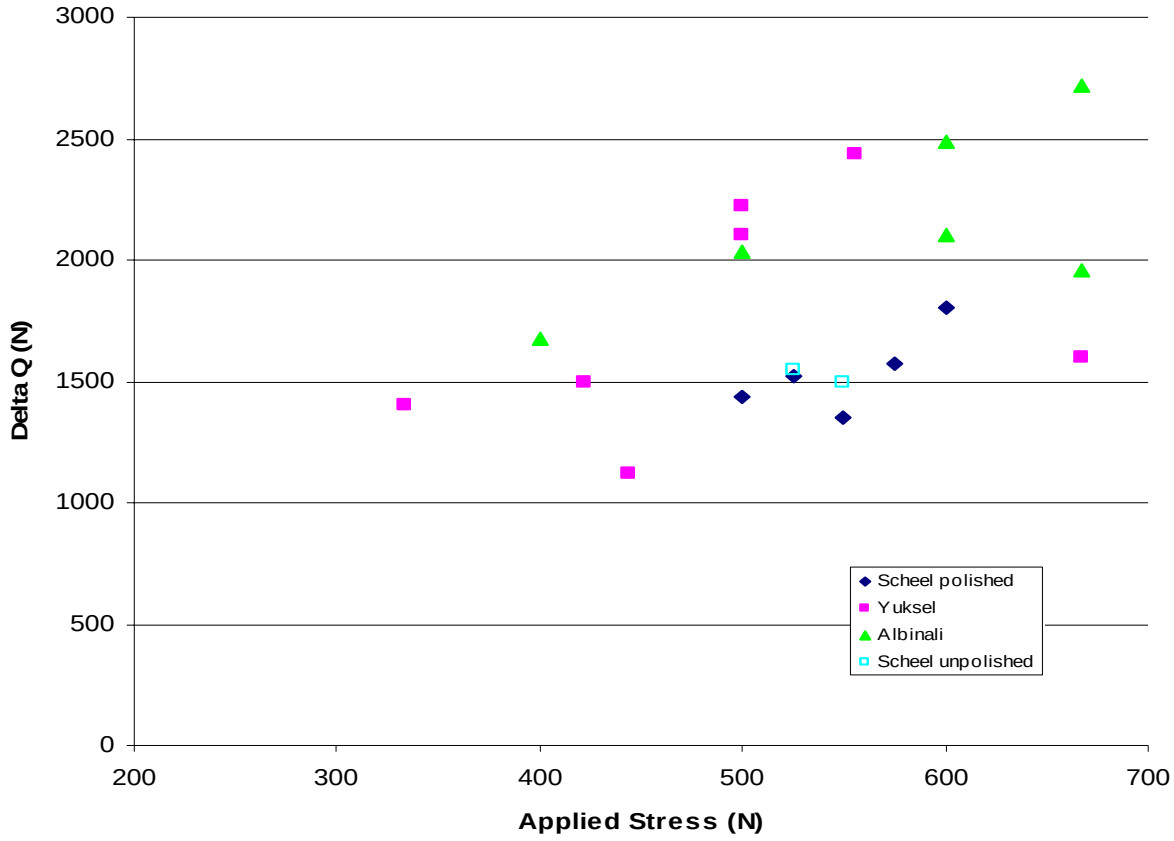

Figure 4.6. ΔQ as it varies with maximum applied stress, σ_{max}.

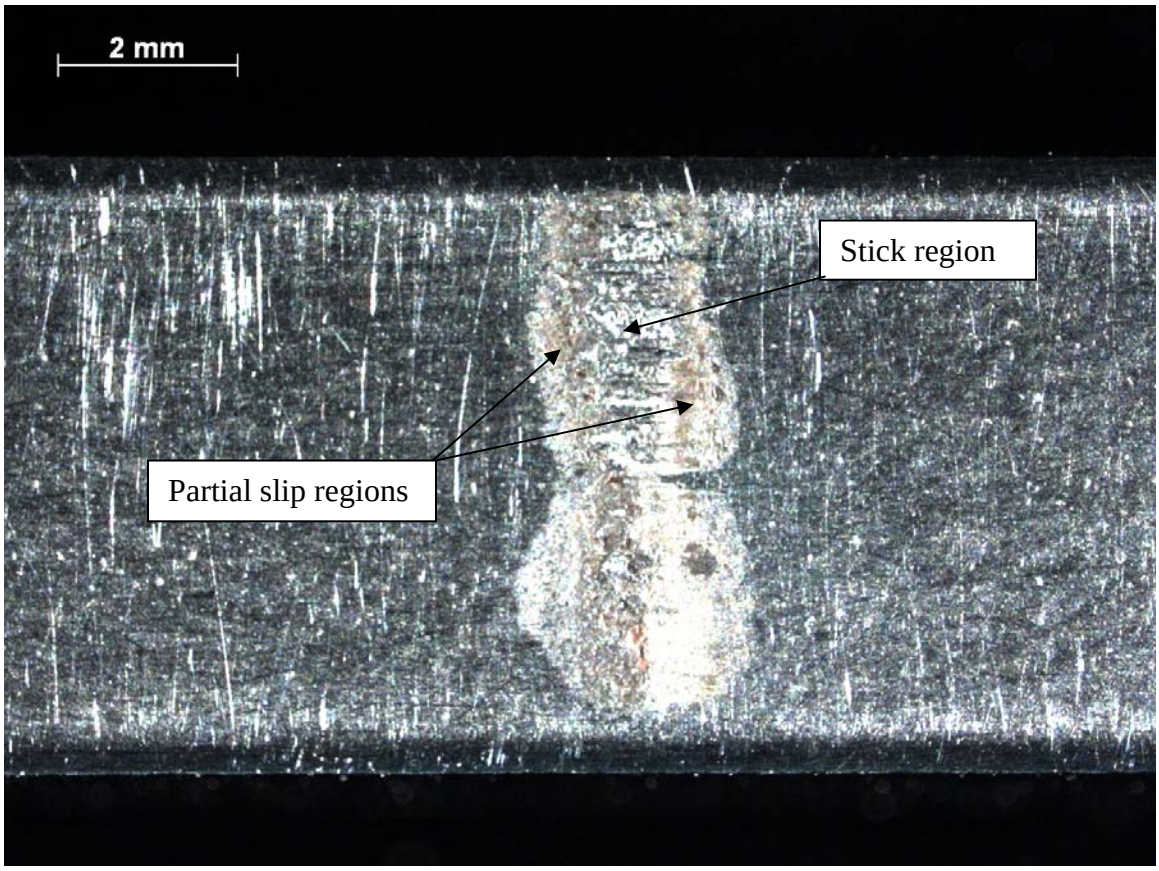

Figure 4.7. Specimen scar indicating partial slip zones and stick zone.

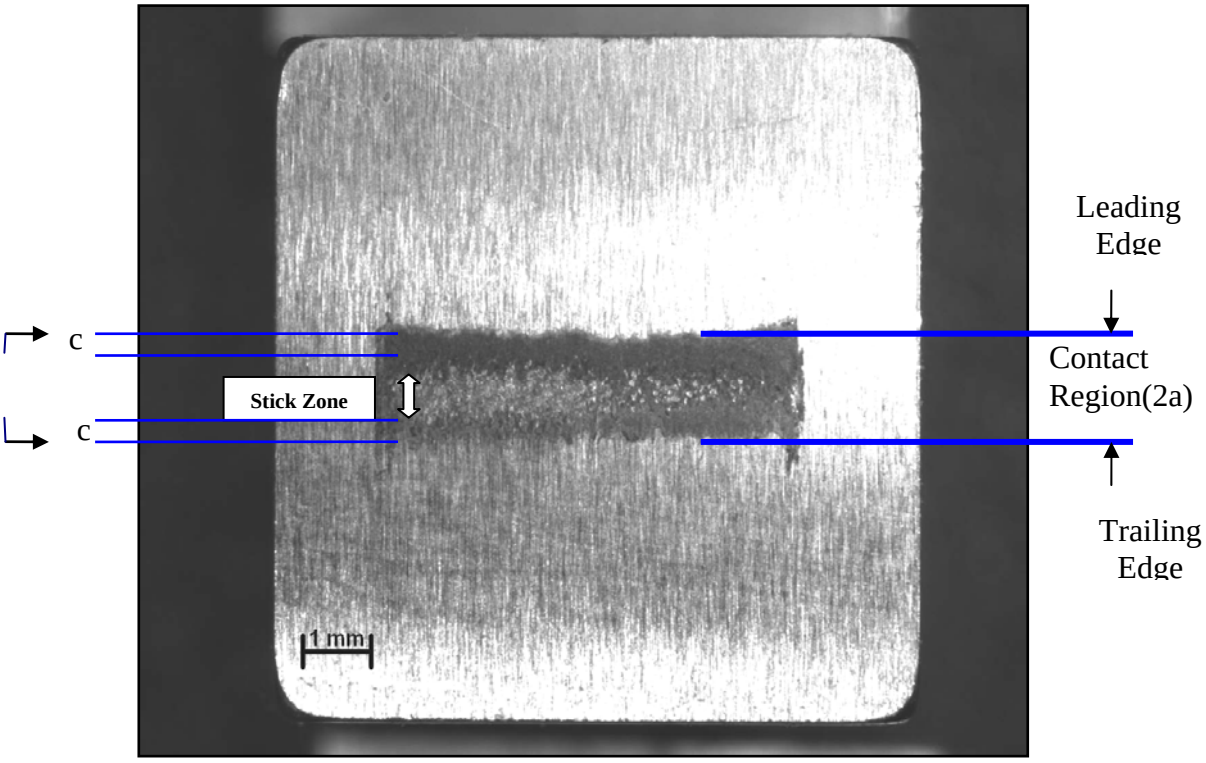

Figure 4.8. Fretting pad surface showing partial slip zones and stick zone.

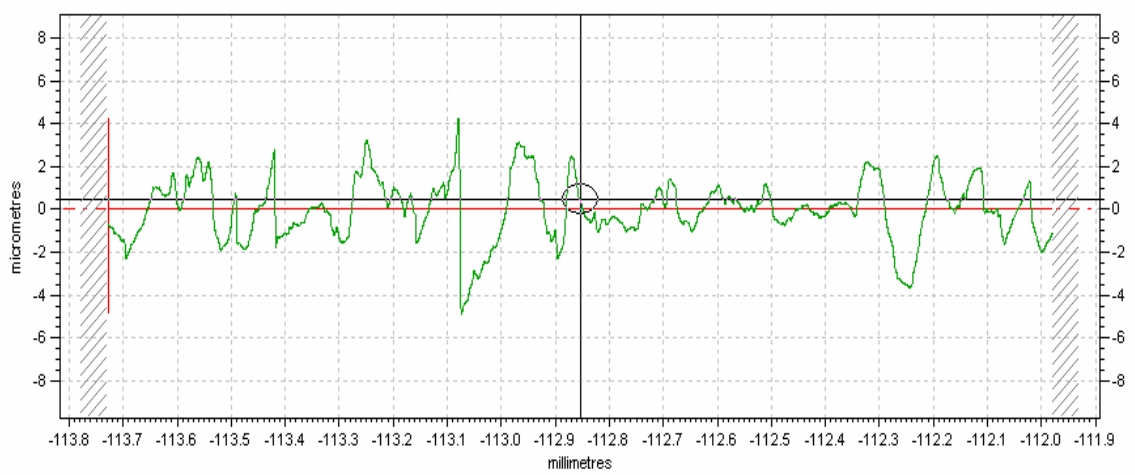

Figure 4.9. Surface roughness profile of fretting scar for unpolished specimen.

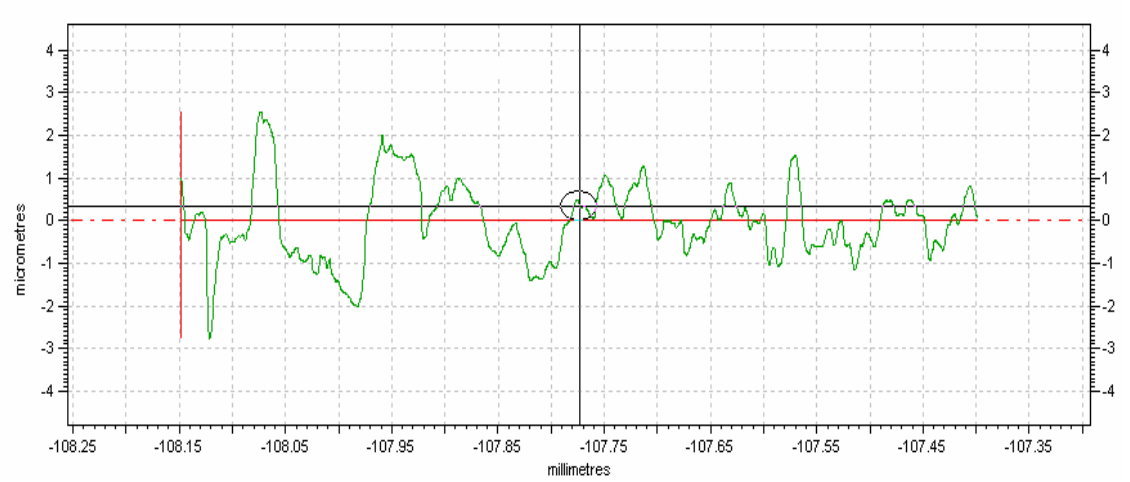

Figure 4.10. Surface roughness profile of fretting scar for polished specimen.

Table 4.1. Surface roughness measurements (micrometers).

	Before Fretting	**After Fretting**
Polished	0.0776	0.8809
Unpolished	1.0953	1.3941

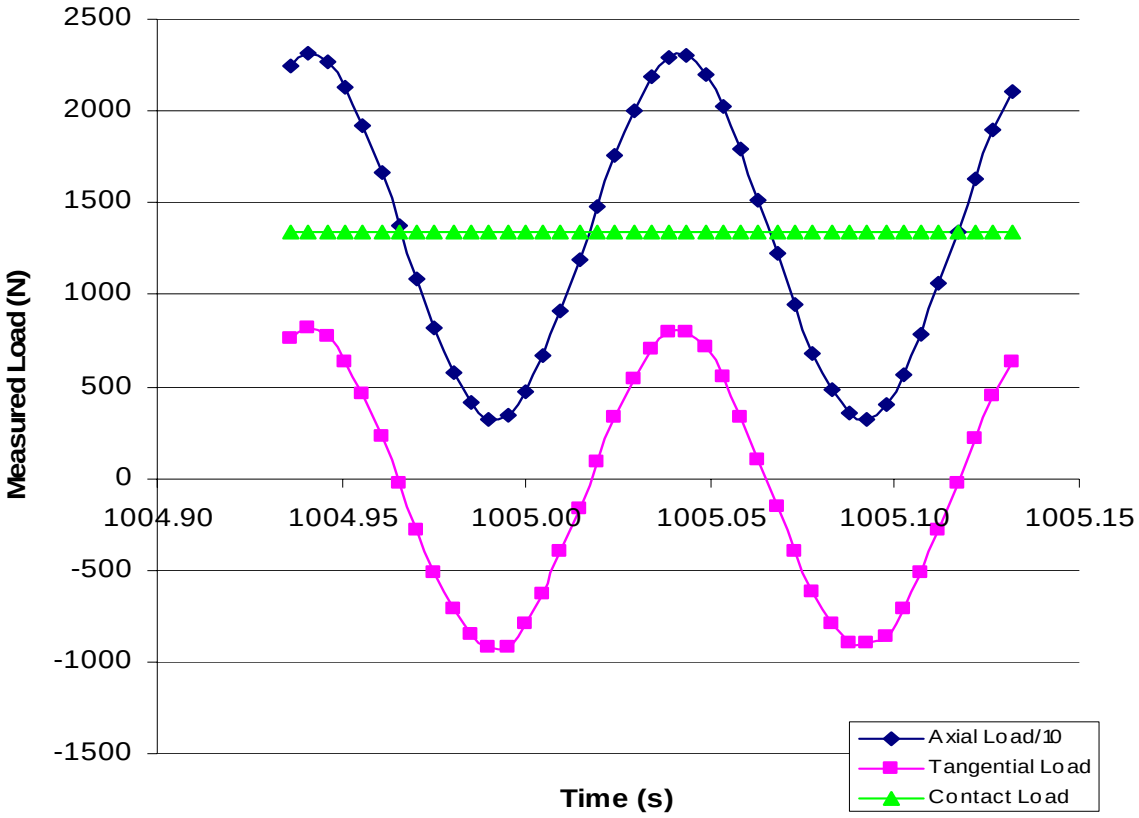

Figure 4.11. Plot illustrating how loads vary with time.

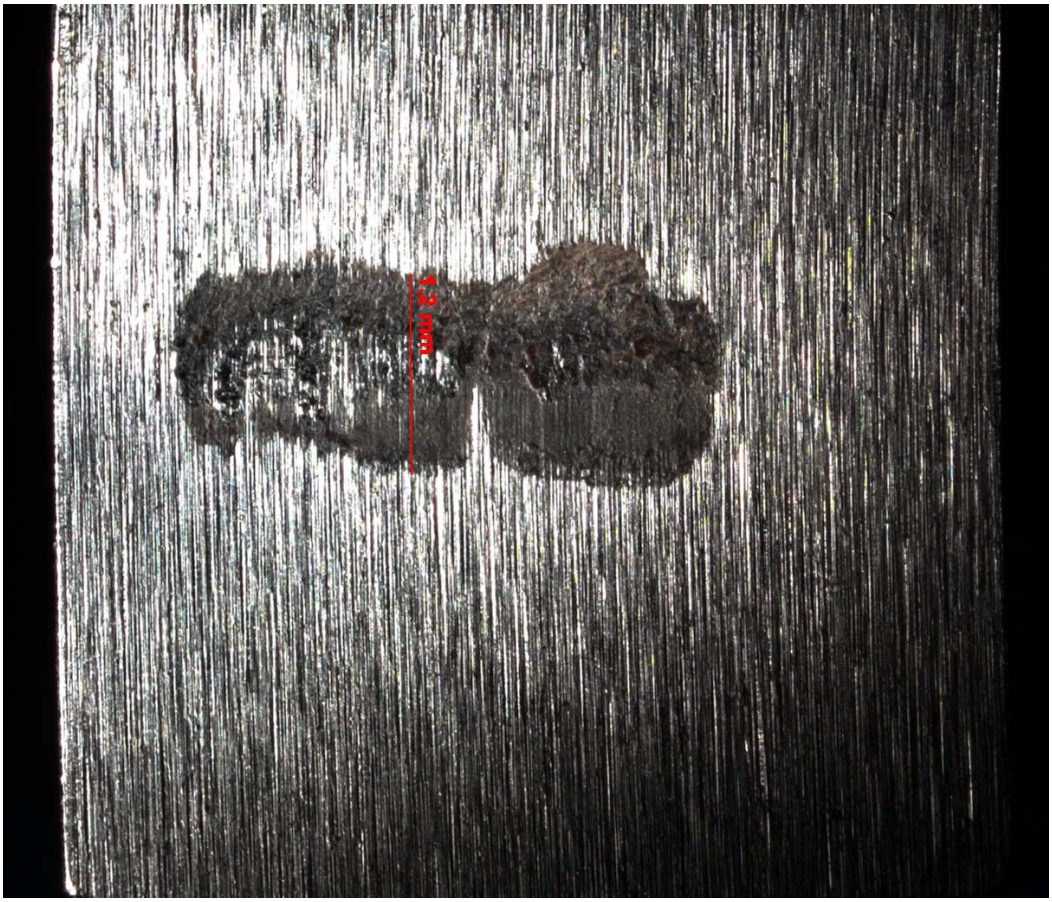

Figure. 4.12. Measured contact width of fretting pad scar.

Table 4.2. Summary of previous research results by Albinali [10] and Yuksel [3].

Researcher Name	Test #	Shot peened (Almen)	σ_{max} (MPa)	σ_{min} (Mpa)	$\Delta\sigma$ (Mpa)	σ_{eff} (Mpa)	Q_{max} (N)	Q_{min} (N)	N_f (Cycles)
Albinali	1	4A	666.66	66.66	600	635.8	1490	-465	9.27e5
Albinali	2	4A	500	50	450	476.85	1364	-666	1.95e6
Albinali	3	4A	400	40	360	381.48	1013	-663	5.22e6
Albinali	4	4A	600	60	540	572.22	1847	-640	7.30e4
Yuksel	5	7A	666.66	66.66	600	635.8	1013	-583	6.25e4
Yuksel	6	7A	555	55	500	529.54	1643	-793	1.24e5
Yuksel	7	7A	500	50	450	476.85	1483	-741	1.56e5
Yuksel	8	7A	444.44	44.44	400	423.86	632	-484	2.42e6
Yuksel	9	7A	422.22	42.22	380	402.67	917	-577	3.56e6
Albinali	10	10A	666.66	66.66	600	635.8	1953	-768	1.62e5
Albinali	11	10A	600	60	540	572.22	1489	-615	2.47e5

Table 4.3. Table of current research results.

Test #	**Peening Intensity** (Almen)	σ_{max} (MPa)	σ_{min} (MPa)	**R** -	σ_{eff} (MPa)	**Q_{max}** (N)	**Q_{min}** (N)	**Nf** (cycles)
1	7A	500	50	0.1	476.85	610	-830	2.75E+06
2	7A	600	60	0.1	572.22	820	-980	2.00E+05
3	7A	550	55	0.1	524.53	640	-710	6.10E+04
4	7A	575	57.5	0.1	548.37	725	-850	3.13E+05
5*	7A	550	55	0.1	524.53	625	-875	5.20E+05
6	7A	525	52.5	0.1	500.69	600	-925	6.65E+05
7*	7A	525	52.5	0.1	500.69	600	-950	2.99E+05

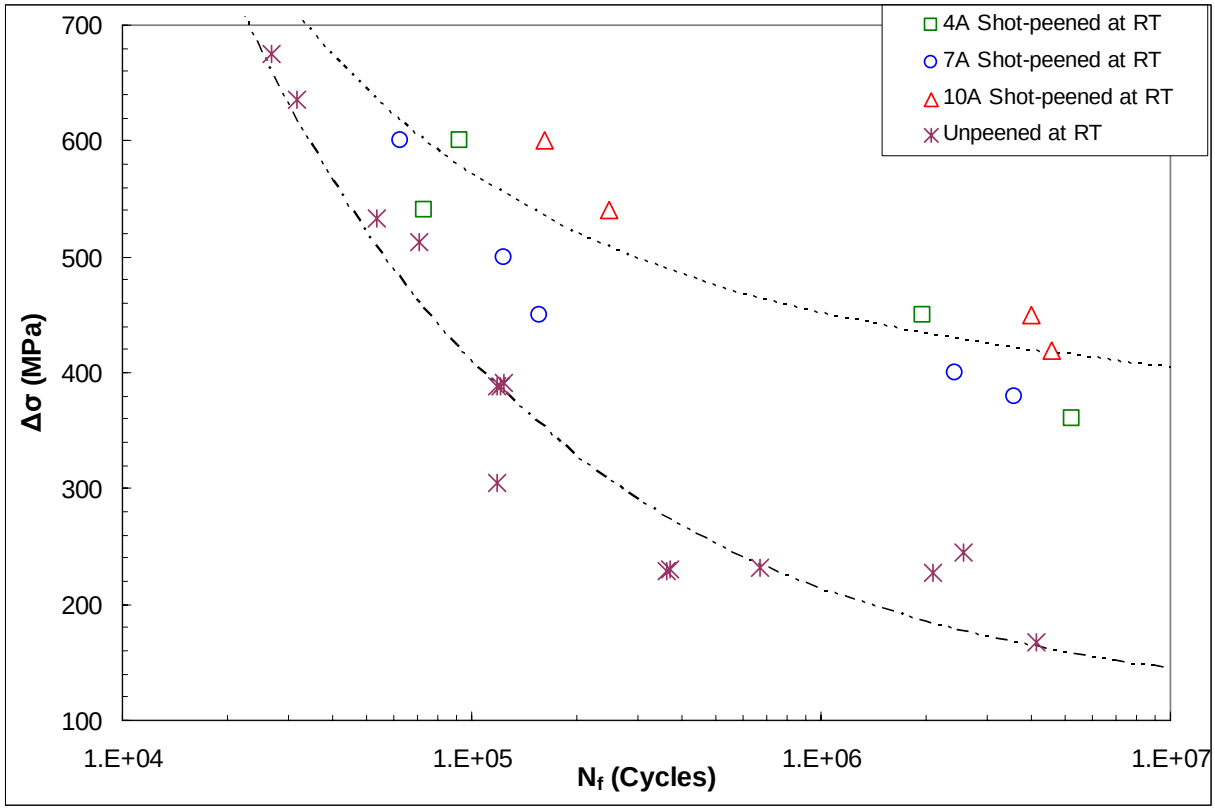

Figure. 4.13. Albinali's Comparison of $\Delta\sigma$-N_f for peened and unpeened specimens [10].

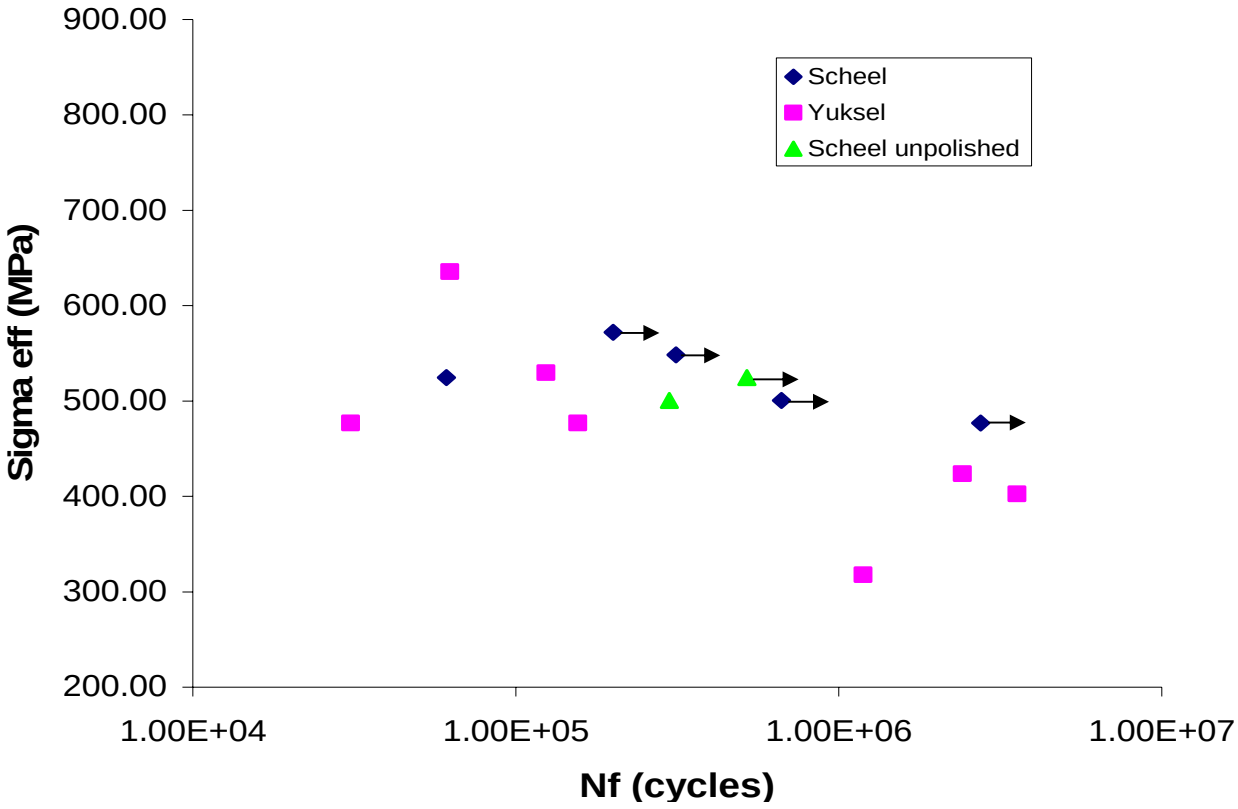

Figure 4.14. Current Data compared with results from Yuksel [3].

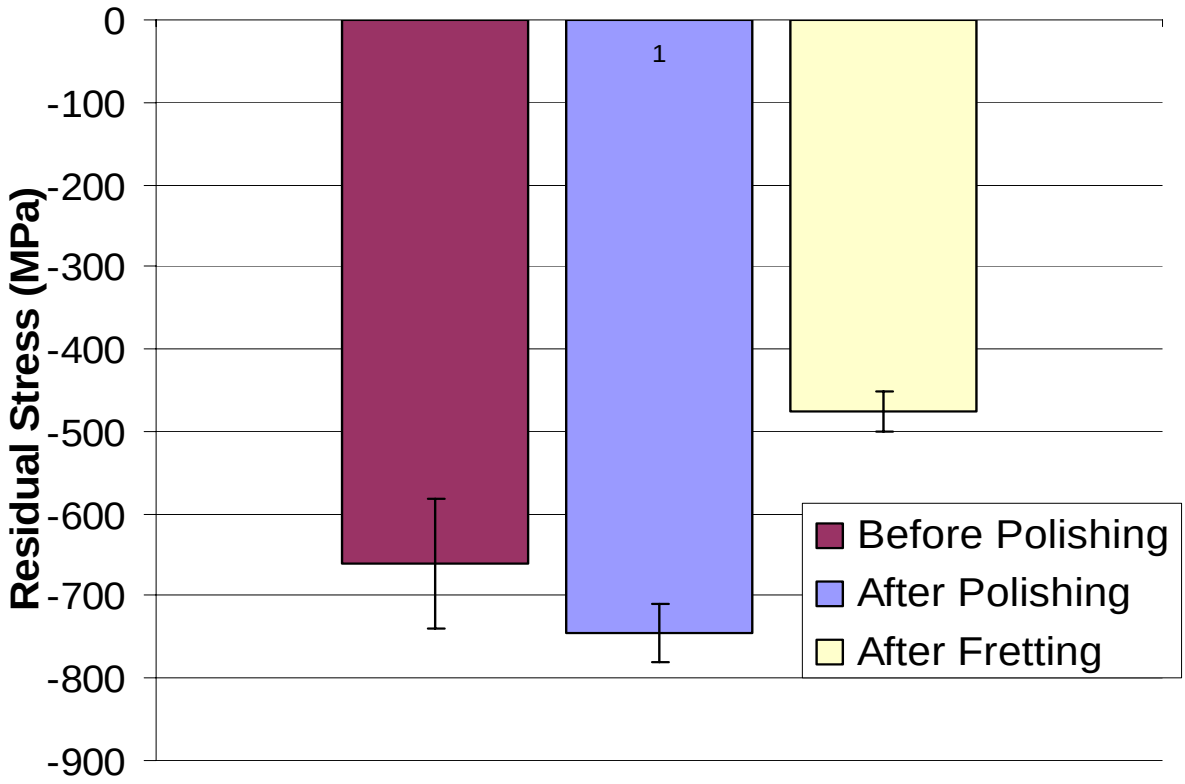

Figure 4.15. Residual stress measurements.

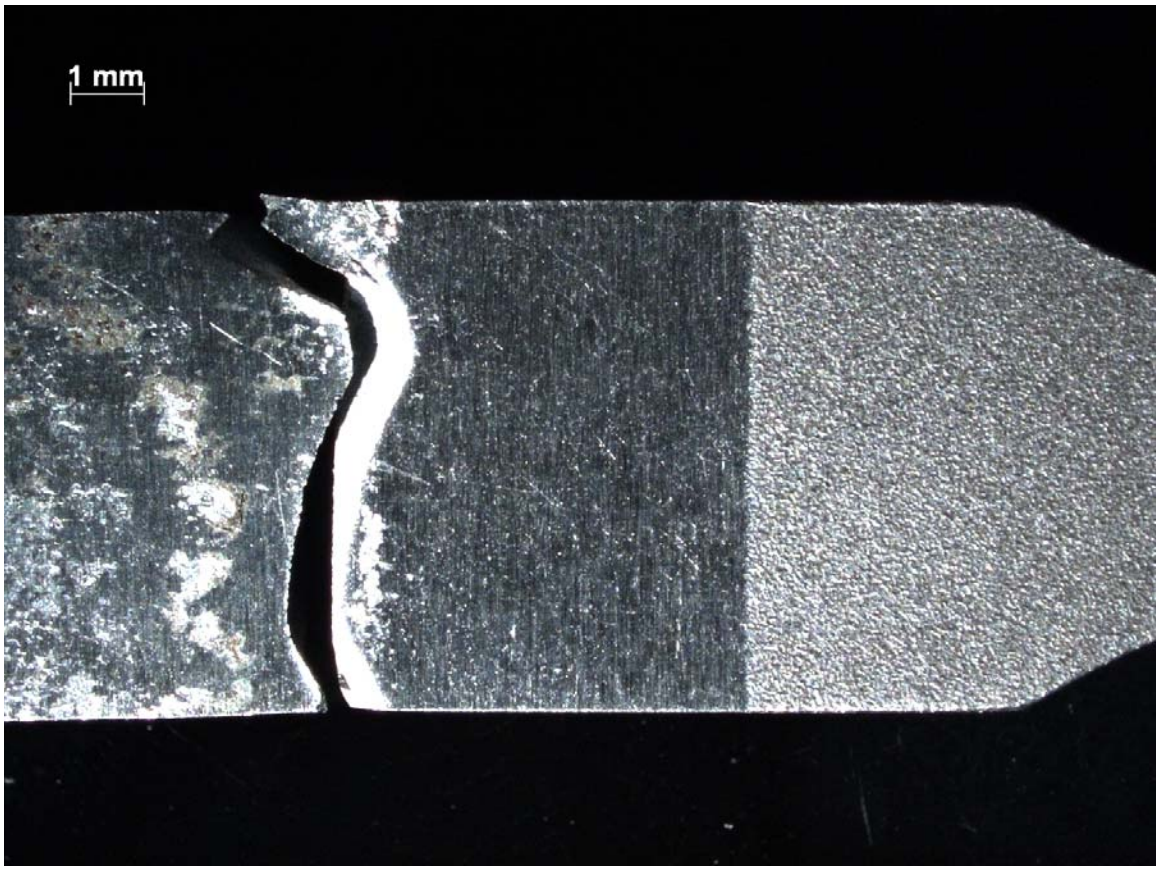

Figure 4.16. Typical fracture location for specimens used in current research.

5 Conclusions & Summary

Equation Section 5

5.1 Summary

The shot-peening process, though one of the most beneficial techniques in prolonging fatigue life due to fretting, creates a textured surface that may lead to problems on the micro level. This research was done in an attempt to further improve the peening process by examining the effects of another surface treatment to be used in conjunction, surface polishing. The textured surface created by the shot-peening process can easily be seen with the naked eye. This rough surface may have contained sharp corners that acted as stress risers, which are more highly prone to crack initiation. Hand polishing the specimens after they were peened was done to remove approximately 25 microns of material from the surface to remove all stress risers while preserving the beneficial residual stresses created by peening. Experiments designed to simulate fretting fatigue similar to previous research were conducted and compared to the results of this research.

Seven experiments were conducted using titanium allow Ti-6Al-4V, shot peened using 7A intensity. Five of these specimens were hand polished after peening and two were left unpolished. Specimen cross-sections were 6.35 mm square. Fretting fatigue tests were conducted over a range of maximum stresses, $\sigma_{\max} = 500 - 600 MPa$ with a constant stress ratio of R = 0.1. All tests were run at ambient air temperature. Stress levels were continually recorded until the specimen fractured. Once it was established that the fretting fatigue condition had been met, a profilometer and optical microscope were used to examine surface roughnesses and certain characteristics of the contact scars.

Problems were encountered during the experimental procedure in that a number of specimens did not fracture on the fretting surface, but instead fractured on the gripping section of the specimen as shown in Fig. 4.13. Due to time constraints, additional testing could not be completed nor could further analysis be conducted on the results obtained.

5.2 Conclusions

Much of the data, once analyzed showed consistent results to previous research, helping to strengthen the validity of certain concepts. Current results were comparable to past research results of shot-peened specimens and thus were consistent with the idea that shot-peening is one of the most effective means of improving fretting fatigue life. On the other hand, certain experimental setbacks were encountered that impeded the analytical process and made interpretation of results the more difficult and uncertain. Be that as it may, data yielded a number of expected results that indicated that the fretting process was proceeding as intended. Figures 4.4 – 4.6 and Fig. 4.9 were used to show that the experiments were running correctly and that the desired conditions were being achieved. Figures 4.7 and 4.8 showed the contact surfaces on both specimen and fretting pad and showed the partial slip zones and stick zone characteristic of fretting fatigue. Below are those things most significantly concluded from this research:

1) Results from the current experimentation show that, though trends on the S-N curve indicate a slight rise in fatigue life of shot-peened and polished specimens when compared to peened but unpolished specimens, due to the uncertainty in fatigue life prediction and the general scatter of data associated with that uncertainty, it cannot be concluded that the polishing process improves fatigue life under fretting conditions.

2) The fretting fatigue conditions being sought during experimentation, that is the partial slip condition, was achieved quicker with the polished specimen than with the unpolished specimen. This was shown with both hysteresis loops and tangential load trends.

3) Profilometer measurements showed that the fretting scars created, regardless of the initial surface condition of the specimens, had surface roughness values that were similar. That is, the roughness profiles of the fretting scars created on the polished and unpolished surfaces did not differ significantly.

4) Furthermore, these surface roughness values were very similar to the roughness of the shot-peened surface before fretting occurred.

This revealed that any potential benefits from the polishing process were not maintained. Polishing was thought to eliminate any stress concentration that may have developed from shot peening process. However, surface roughness measurements showed that scarring created by the fretting process left a surface as rough as that created by shot-peening. Logically, this would mean that the same potential for unwanted stress concentration would exist and any potential benefit from polishing would be negated.

However, it was shown that, though fatigue life was not conclusively improved, it certainly was not hindered. Given the limitations of this research, a number of things were not addressed that rightfully should be, including the use of more intensive analysis techniques as well as addressing the economic and manufacturing feasibility of polishing.

5.3 Future Work

It is readily apparent that more work needs to be done. Time did not permit some of the more in depth analysis of the specimen behavior or fracture surfaces, such as Finite Element Analysis, Scanning Electron Microscopy (SEM), X-ray diffraction or determination of the crack initiation location or crack orientation. Additionally, the setbacks encountered with the gripping pads of the MTS machine hindered progress. It is recommended that the hypothesis that polishing a shot-peened surface will improve the fretting fatigue life of Ti-6Al-4V continue to be tested. More experiments should be run and more in depth analysis completed with the use of SEM and analysis tools such as FEA. If it can be concluded that an improvement has been made in the fretting fatigue life of the alloy in ambient conditions, then further testing should be done to see how the process holds up in more hostile environments, such as elevated temperatures or seawater conditions.

Bibliography

1. Hills, D. and D. Nowell. *Mechanics of Fretting Fatigue,* Kluwer Academic Publishers, Netherlands, 1994.

2. Jutte, A.J. "Effect of a Variable Contact Load on FrettingFatigue Behavior of Ti-6Al-4V," MS Thesis AFIT/GAE/ENY/04-M09, Air Force Institute of Technology, Wright-Patterson Air Forec Base, Ohio, March 2004.

3. Waterhouse, R.B. "Fretting Fatigue," *International Materials review*, 37: 77-97 (1992)

4. Callister, William D. *Materials Science and Engineering; an Introduction*. 6th ed. Hoboken, NJ: John Wiley & Sons, Inc., 2003. 219.

5. Yuksel, H.I. "Effects of Shop-peening on High Cycle Fretting Fatigue Behavior of Ti-6Al-4V," MS Thesis AFIT/GAE/ENY/02-12. Air Force Institute of Technology (AU), Wright-Patterson Air Force Base, OH, December 2002.

6. H. Lee, O. Jin and S. Mall. "Fretting Fatigue Behavior of Shot-peened Ti-6Al-4V at Room and Elevated Temperature," *Fatigue Fract Engng Master Struct*, 26: 1-12 (2003).

7. Waterhouse, R.B. *Fretting Fatigue*. Oxford: Pergamon Press Ltd, 1972.

8. Lee, C. "Effect of Variable Contact Load on Fretting FATIGUE Behavior of Shot-peened and Un-peened Titanium Alloy Ti-6Al-4V," MS Thesis AFIT/GAE/ENY/04-D01, Air Force Institute of Technology, Wright-Patterson Air Force Base, December 2004.

9. Lykins, C.D., S. Mall and Douglas. "An Investigation of Fretting Fatigue Crack Initiation Behavior of the Titanium Alloy Ti-6Al-4V," PhD dissertation, University of Dayton, December 1999.

10. Iyer, K. and S. Mall. "Analysis of Contact Pressure and Stress Amplitude Effects on Fretting Fatigue Life," *Journal of Engineering Materials and Technology*, 123:85-93 (January 2001).

11. Namjoshi, S., Mall, S., Jain, V. and Jin, O., "Fretting Fatigue Crack Initiation Mechanisms in Ti-6Al-4V," *Fatigue and Fracture of Engineering Material and Structures*, Vol. 25, No. 10, 955-964, Oct 2002.

12. Namjoshi, S., S. Mall, V.K. Jain and O. Jain. "Effects of Process Variables on Fretting Fatigue Crack Initiation in Ti-6Al-4V," Journal of Strain Analysis, 37, No.6: 535-542 (2002).

13. Iyer, K. and S. Mall. “Effects of Cyclic Frequency and Contact Pressure on Fretting Fatigue under Two-Level Block Loading,” Fatigue Fract. Engng. Mater. Struct., 23: 335-346 (2000).

14. Lee, H. and S. Mall. “Stress Relaxation Behavior of Shot-peened Ti-6Al-4V Under Fretting Fatigue at Elevated Temperature,” *Materials Science and Engineering* A366: 412-420 (2004).

15. Poon, C. and D.W. Hoeppner. “The Effect of Environment on the Mechanism of Fretting Fatigue,” *Wear*, 52: 175-191 (1979).

16. Conner, B.P., A.L. Hutson and L. Chambon. “Observations of Fretting Fatigue Micro-Damage of Ti-6Al-4V,” Wear, 255: 259-268 (2003).

17. Endo, K. and H. Goto. “Effects of Environment of Fretting Fatigue,” Wear, 48: 347-367 (1978).

18. Waterhouse, R.B. and M.K. Dutta. “The Fretting Fatigue of Titanium and Ssome Titanium Alloys in a Corrosive Environment,” *Wear*, 25:171-175 (1973).

19. Wharton, M.H. and R.B. Waterhouse. “Environmental Effects oin the Fretting Fatigue of Ti-6Al-4V,” Wear, 62: 287-297 (1980).

20. Lykins, C. D., S. Mall and V. K. Jain, *An evaluation of Parameters of Predicting Fretting Fatigue Crack Initiation*, International Journal of Fatigue, Vol. 22, 703-716, 2000.

21. Albinali, S. “Effects of Temperature and Shot-peening Intensity on Fretting Fatigue Behavior of Titanium Alloy Ti-6Al-4V,” MS Thesis AFIT/GAE/ENY/05-M25, Air Force Institute of Technology, Wright-Patterson Air Force Base, Ohio, March 2005.

22. Mutoh, Y., T. Satoh and E. Tsunoda. *Improving Fretting Fatigue Strength at Elevated Temperatures by Shot-Peening in Steam Turbin Steel*, Standardization of Fretting Fatigue Test Methods and Equipment, ASTM STP 1159, M. Helmi Attia and R.B. Waterhouse, Eds., American Society for Testing and Materials, Philadelphia: 199-209 (1992).

23. S. A. Martinez. “Quantitative Characterization of Fretting Fatigue Damage in Shot-Peened Ti-6Al-4V,” Thesis, University of Dayton, Dayton, OH (August 2004).

24. V. Sabelkin, S.A. Martinez, S. Mall, S. Sathish and M.P. Blodgett. “Effects of Shot-Peening Intensity on Fretting Fatigue Crack Initiation Behavior of Ti-6Al-4V,” Department of Aeronautics and Astronautics, Air Force Institute of Technology, Wright Patterson Air Force Base, Ohio, in press.

25. R. L. Mattson. “Fatigue: Residual Stress and Cold Working,” International Conference on Fatigue of Metals, *Institute of Mechanical Engineers*, 593-603 (1956).

26. C. D. Lykins, *An Investigation of Fretting Fatigue Crack Initiation Behavior on the Titanium Alloy Ti-6Al-4V*, Dissertation.

27. Lykins, C. D., S. Mall and V. K. Jain, "Combined Experimental-numerical Investigation of Fretting Fatigue Crack Initiation," International Journal of Fatigue, Vol. 23, No. 9, 703-711, Sept. 2001.

28. Coffin, L. Jr., "A study of the Effects of Cyclic Thermal Stresses on a Ductile Metal," Trans. ASME, 76: 931-950 (1954).

29. W. J. Harris, *The Influence of Fretting on Fatigue*, AGARD Advisory Group for Aerospace Research and Development, Advisory Report 8, 1967.

30. Hoeppner, D. and G. Goss, *A Fretting Fatigue Damage Threshold Concept*, Wear, Vol. 27, 1974, 61-70.

31. Lindley, T. and K. Nix, *The Role of Fretting in the Initiation and Early Growth of Fatigue Cracks in Turbo Generator Materials*, Muliaxial Fatigue, ASTM, 1985, 340-360.

32. Ruiz, C., P. Boddington and K. Chen, *An Investigation of Fagigue and Fretting in a Dovetail Joint*, Experimental Mechanics, 1984, Vol. 24, No. 3, 208-217.

33. Lykins, C. D., S. Mall and V. K. Jain, *An evaluation of Parameters of Predicting Fretting Fatigue Crack Initiation*, International Journal of Fatigue, Vol. 22, 703-716, 2000.

34. A. Elkholy, *Fretting Fatigue in Elastic Contacts Due to Tangential Micromotion*, Tribology International, 1996, Vol. 29, No. 4, 256-273.

REPORT DOCUMENTATION PAGE

Form Approved
OMB No. 074-0188

1. REPORT DATE *(DD-MM-YYYY)*	**2. REPORT TYPE**	**3. DATES COVERED** *(From – To)*
23-09-2005	**Master's Thesis**	SEP 2005 – SEP 2006

4. TITLE AND SUBTITLE

EFFECTS OF POLISHING SHOT-PEENED SURFACES ON FRETTING FATIGUE BEHAVIOR OF Ti-6Al-4V

5a. CONTRACT NUMBER

5b. GRANT NUMBER

5c. PROGRAM ELEMENT NUMBER

6. AUTHOR(S)

Scheel, Kasey, S., Ensign, USN

5d. PROJECT NUMBER

5e. TASK NUMBER

5f. WORK UNIT NUMBER

7. PERFORMING ORGANIZATION NAMES(S) AND ADDRESS(S)

Air Force Institute of Technology
Graduate School of Engineering and Management (AFIT/EN)
2950 Hobson Way
WPAFB OH 45433-7765

8. PERFORMING ORGANIZATION REPORT NUMBER

AFIT/GAE/ENY/06-S10

9. SPONSORING/MONITORING AGENCY NAME(S) AND ADDRESS(ES)

AFRL/MLLP
Attn: Dr. Mark Blodgett
Metals, Ceramics and NDE Division
Materials and Manufacturing Directorate
2230 Tenth St., Suite 1 Bldg 655
WPAFB OH 45433 DSN: 785-9799

10. SPONSOR/MONITOR'S ACRONYM(S)

11. SPONSOR/MONITOR'S REPORT NUMBER(S)

12. DISTRIBUTION/AVAILABILITY STATEMENT

APPROVED FOR PUBLIC RELEASE; DISTRIBUTION UNLIMITED.

13. SUPPLEMENTARY NOTES

14. ABSTRACT

The research of this thesis was done to investigate the effects of polishing a shot-peened specimen of Ti-6Al-4V on the fretting fatigue life of that specimen. The shot-peening process, though one of the most beneficial techniques in prolonging fretting fatigue life, creates a textured surface that may lead to problems on the micro level. This research was done in an attempt to further improve the peening process by examining the effects of another surface treatment to be used in conjunction, surface polishing. The rough peened surface may contain abrupt changes in surface geometry that act as stress risers, which are more highly prone to crack initiation. Specimens were hand polished after they were peened to remove approximately 25 microns of material from the surface to remove all stress risers while preserving the beneficial residual stresses created by peening. Experiments designed to simulate fretting fatigue similar to previous research were conducted until specimens fractured. Seven experiments were conducted using titanium allow Ti-6Al-4V, shot peened using 7A intensity. All tests were run at ambient air temperature. Fatigue parameters, such as stress range and effective stress, were analyzed. Fretting fatigue conditions were determined and surface roughness measurements of polished and unpolished specimens were taken. It was concluded that, though fatigue life was improved over that of un-peened specimens, the polishing process did not improve the fretting fatigue life of the alloy.

15. SUBJECT TERMS

Fretting fatigue, titanium alloy, Ti-6Al-4V, shot-peening, polishing

16. SECURITY CLASSIFICATION OF:			**17. LIMITATION OF ABSTRACT**	**18. NUMBER OF PAGES**	**19a. NAME OF RESPONSIBLE PERSON**
REPORT	**ABSTRACT**	**c. THIS PAGE**			Dr. Shankar Mall
U	**U**	**U**	**UU**	84	**19b. TELEPHONE NUMBER** *(Include area code)* (937) 255-3636, ext 4587; e-mail: Shankar.Mall@afit.edu